Anuário do Instituto de Geociências
Universidade Federal do Rio de Janeiro
https://revistas.ufrj.br/index.php/aigeo/

ISSN 0101-9759
e-ISSN 1982-3908

GEOLOGY

Biostratigraphy and Paleoenvironmental Characterization of the Lower Cretaceous Codó and Itapecuru Formations (Aptian–Albian, Parnaíba Basin, Brazil)

Bioestratigrafia e Caracterização Paleoambiental das Formações Codó e Itapecuru (Aptiano–Albiano da Bacia do Parnaíba, Brasil)

Lucas Lage Machado[1], Cecília de Lima Barros[1], Aristóteles de Moraes Rios-Netto[1], Benjamin Sames[2], Silvia Clara Silva[1], João Graciano Mendonça Filho[3], Joalice de Oliveira Mendonça[3] & Danielle Marques-Lima[3]

[1] Universidade Federal do Rio de Janeiro, Instituto de Geociências, Departamento de Geologia, Laboratório de Micropaleontologia Aplicada (MicrA), Rio de Janeiro, RJ, Brasil
[2] University of Vienna, Department of Geology, Vienna, Austria
[3] Universidade Federal do Rio de Janeiro, Instituto de Geociências, Departamento de Geologia, Laboratório de Palinofácies e Fácies Orgânica (LAFO), Rio de Janeiro, RJ, Brasil

E-mails: lucaslage@geologia.ufrj.br; ceciliabarros@geologia.ufrj.br; rios.netto@geologia.ufrj.br; benjamin.sames@univie.ac.at; silviaclara@geologia.ufrj.br; graciano@geologia.ufrj.br; joalice@lafo.geologia.ufrj.br; danimarques@lafo.geologia.ufrj.br

Abstract

The Parnaíba Basin is a Brazilian intracratonic basin located in the North and Northeastern regions of the country. Its Cretaceous succession holds significant scientific and economic importance, as it is correlated with the Aptian Pre-Salt deposits of Brazil and contains early records of marine incursions associated with the opening of the South Atlantic Ocean. This study aims to identify ostracods and organic matter constituents recovered from samples of a fully cored geological section recently drilled in the Parnaíba Basin (2-CO-1-MA borehole, within the interval corresponding to the Codó and Itapecuru formations). The objectives are to establish an ostracod-based biostratigraphic framework for this section, and to infer paleoenvironmental conditions through the integrated analysis of ostracods and palynofacies. Species of the ostracod genera *Damonella* and *Pattersoncypris* were identified, alongside megaspores, termite coprolites, fish fragments, gastropoda and foraminifera, characterizing a low diversity fauna and flora assemblage. In addition, the palynofacies revealed the presence of phytoclasts, amorphous organic matter, and palynomorphs within the studied samples. Four microfossil associations and three palynofacies were identified in the studied section, which is constrained to the upper Aptian. The evolution of the sedimentary succession is marked by a range of paleoenvironments, including lacustrine, brackish lacustrine, evaporitic-sabkha, fluvial, lagoonal, and fluvio-deltaic settings.

Keywords: Ostracods; Palynofacies; Biostratigraphy

Resumo

A Bacia do Parnaíba é uma bacia intracratônica brasileira localizada nas regiões Norte e Nordeste do país. Sua sequência cretácea constitui grande relevância científica e econômica, pois correlaciona-se aos depósitos aptianos do Pré-Sal e inclui registros de incursões marinhas relacionadas à abertura do Atlântico Sul. Este trabalho tem como objetivo identificar ostracodes e constituintes da matéria orgânica recuperados de amostras de uma seção geológica completa, recentemente perfurada na bacia (poço 2-CO-1-MA, intervalo identificado como formações Codó e Itapecuru), estabelecer um arcabouço bioestratigráfico baseada em ostracodes para essa seção e realizar inferências paleoambientais com base na integração da análise de ostracodes e palinofácies. Espécies dos gêneros de ostracodes *Damonella* e *Pattersoncypris* foram registradas juntamente com megásporos, coprólitos de cupins, fragmentos de peixes, gastropoda e foraminifera, caracterizando uma fauna e flora de baixa diversidade. Fitoclastos, matéria orgânica amorfa e palinomorfos foram identificados nas amostras estudadas. Quatro associações de microfósseis e três palinofácies são descritas. A seção estudada é atribuída ao Aptiano superior e caracterizada por paleoambientes lacustres, lacustres salobros, sabbkha-evaporíticos, fluviais, lagunares e flúvio-deltaicos.

Palavras-chave: Ostracodes; Palinofácies; Bioestratigrafia

Received: 18 March 2025; Accepted: 03 July 2025

1 Introduction

The fragmentation of Gondwana during the Early Cretaceous played a key role in the development of the South Atlantic Ocean and, simultaneously, influenced the deposition of Cretaceous sediments in the Parnaíba Basin (Vaz *et al.* 2007). Through ostracod and palynomorph biozones, as well as clay mineral assemblage, the Cretaceous sequence, particularly the Codó Formation, has been correlated with the Pre-Salt interval in Brazilian marginal basins, serving as a readily accessible analogue for study (Maizatto *et al.* 2011; Poropat & Colin 2012a; Salgado-Campos *et al.* 2022). Paleontological indicators—such as dinoflagellate cysts and isopods—and geochemical evidence, including hydrocarbon biomarkers, have been interpreted in the Codó Formation. While not conclusive, these findings align with similar data from other sedimentary basins, including São Luís, Araripe, and Sergipe, and lend support to the hypothesis of a Cretaceous seaway in Northeastern Brazil (Antonioli & Arai 2002; Arai 2014; Bastos *et al.* 2020; 2022; Lindoso *et al.* 2013). Therefore, the detailed characterization of the paleoenvironments in the Parnaíba Basin during the Aptian–Albian is important due to the possible paleogeographic implications and is relevant for the study of Pre-Salt analogues.

The Cretaceous succession of the Parnaíba Basin includes the Codó, Itapecuru, Corda and Grajaú formations, deposited during the Aptian–Albian (Vaz *et al.* 2007). The Codó Formation is referred in the literature as an inland restricted lacustrine system, with variable marine influence (Batista 1992; Bahniuk *et al.* 2015; Mendes 2007; Mesner & Wooldridge 1964; Paz *et al.* 2005; Rossetti *et al.* 2004; Salgado-Campos *et al.* 2022). The Itapecuru Formation is considered to have been deposited in fluvial and estuarine settings (Anaisse Júnior *et al.* 2001; Corrêa-Martins *et al.* 2019; Ferreira *et al.* 2020).

Ostracods are generally considered to have good applicability as indicators of paleoecological parameters, such as salinity and oxygen levels for various aquatic paleoenvironments, due to differences in adaptability for each genus and to the possibility of taphonomical and ontogenetic approaches (Boomer *et al.* 2003; Carbonel 1988; Neale 1988). Among the extensive geological literature available for the Cretaceous in the Parnaíba Basin, however, relatively few studies have focused on ostracod occurrences (Barros *et al.* 2022; Maizatto *et al.* 2011; Ramos *et al.* 2006). Additionally, despite the significant relevance and substantial contributions of existing ostracod studies, previously studied material has often presented limitations, such as difficulties in correlating with other stratigraphic sections or poor preservation of recovered specimens, highlighting the need for further investigations.

Palynofacies and organic facies analysis provide important information related to kerogen abundance and origin, serving as an important tool for the study of depositional paleoenvironments (Batten & Stead 2005; Traverse 2007; Tyson *et al.* 2005). Therefore, improvements in the characterization of organic composition are particularly beneficial for the Codó and Itapecuru formations, as few authors focused on this subject (Marques-Lima *et al.* 2023; Neves 2007).

This study is based on a recently drilled and fully recovered section from the Parnaíba Basin. It aims to identify ostracods from core samples, establish an ostracod-based biostratigraphic framework and characterize the organic matter record through the use of organic petrography and geochemical techniques. The integration of ostracod analysis and palynofacies contributes to a more comprehensive understanding of the Aptian–Albian interval in the Parnaíba Basin and supports refined palaeoenvironmental interpretations for this stratigraphic succession.

2 Geological Setting

The Parnaíba Basin (Figure 1A) is bordered by the São Luís and Barreirinhas basins, from which it is separated by the Ferrer–Urbano Santos Arch to the north; to the northwest, it is delimited by the Marajó Graben, separated by the Tocantins Arch; and to the south and southeast, it is bounded by Precambrian basement exposures correlated with the Brasília Fold Belt (Cunha 1986).

Formerly known as the Maranhão Basin (Mesner & Wooldridge 1964), it is one of Brazil's largest intracratonic basins, located in the Northern and Northeastern regions of the country (Milani *et al.* 2007). It covers an extensive area of approximately 600,000 km² and preserves a sedimentary and magmatic succession up to 3,500 metres thick, with stratigraphic records spanning from the Silurian to the Cretaceous. This stratigraphic succession, subdivided into five major sequences—Silurian, Devonian, Carboniferous–Triassic, Jurassic, and Cretaceous—rests upon a basement comprising diverse geological units of Archean, Proterozoic, and Cambrian–Ordovician age (Góes & Feijó 1994; Vaz *et al.* 2007).

CC BY

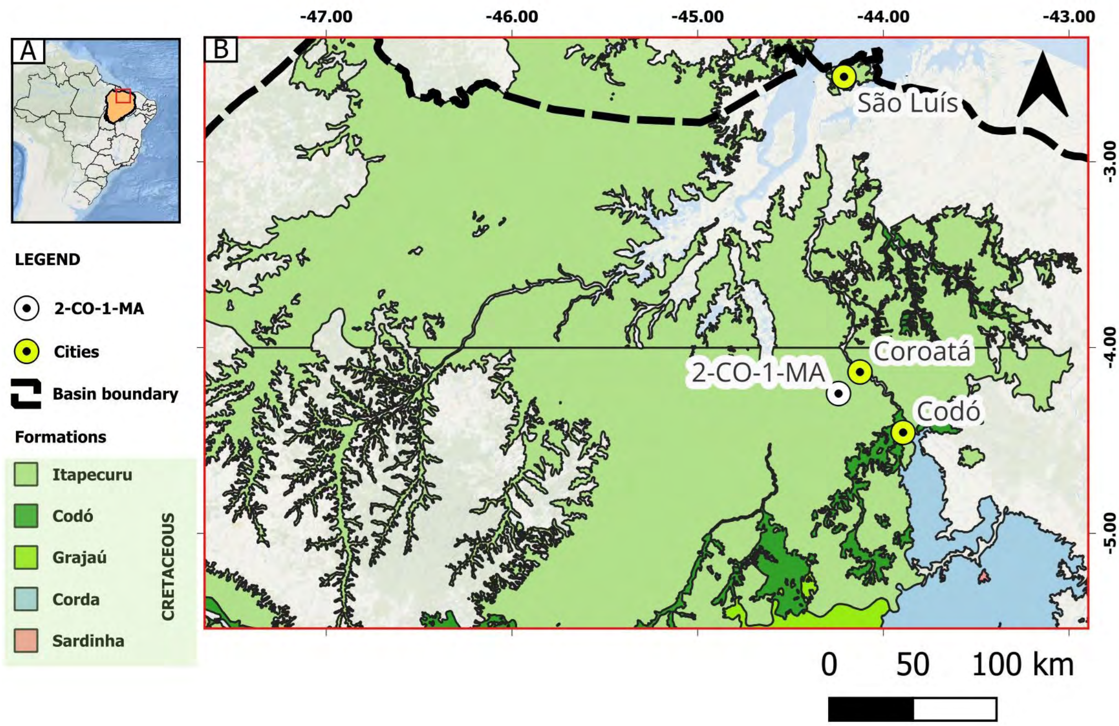

Figure 1 Location map of the study area: A. Geographic map of Brazil, with Parnaíba Basin in orange; B. Geologic map of the northern Parnaíba Basin (Vasconcelos *et al.* 2004), main cities of the studied area, and location of the 2-CO-1-MA borehole.

The Cretaceous succession in the Parnaíba Basin consists of several lithostratigraphic units, including the Corda, Grajaú, Codó, and Itapecuru formations, all of which were deposited under predominantly continental conditions (Góes & Feijó 1994; Vaz *et al.* 2007). This continental sequence rests above Barremian basic igneous rocks of the Sardinha Formation (Vaz *et al.* 2007). Notably, some authors have previously regarded this sequence as a separate sedimentary basin, due to the polycyclic nature of Parnaiba's basin infill, referring to it as the Grajaú Basin (Góes 1995; Góes & Coimbra 1996; Góes & Rossetti 2001).

The Codó Formation is composed of shales, siltstones, sandstones, gypsum, and limestones (Vaz *et al.* 2007). It covers an area of approximately 170,000 km² in the state of Maranhão, reaches a maximum thickness of around 180 meters, and unconformably overlies the Corda Formation (Fernandes & Della Piazza 1978; Vaz *et al.* 2007). According to Mendes (2007), the Codó Formation can be subdivided into two intervals: the lower Codó, interpreted as having been deposited in a closed hypersaline lacustrine system, and the upper Codó, associated with a lacustrine environment influenced by marine incursions. These are delimited by an unconformity identified at the base of a sandstone bed, a proposition that has also been adopted by Bobco *et al.* (2023). Previous studies have identified the P-270 and P-280 palynozones, proposing slightly different chronostratigraphic constraints for the Codó Formation, ranging from the upper Aptian (Batista 1992; Ferreira *et al.* 2020; Lima 1982) to the boundary of Aptian–Albian intervals (Antonioli & Arai 2002; Rossetti *et al.* 2001). Ostracod biostratigraphic studies are less numerous, and all point towards an upper Aptian age, based on the *Cytheridea*? spp. 201–218 Biozone (Barros *et al.* 2022; Maizatto *et al.* 2011; Ramos *et al.* 2006). Facies analyses of the Codó Formation include Paz and Rossetti (2001), who interpreted inland lacustrine paleoenvironments being responsible for the deposition of the entire Codó Formation, which was also supported by strontium isotope ratios (Paz *et al.* 2005). Other studies (*e.g.* Batista 1992; Mendes 2007) identified marine ingressions in some levels and interpreted lacustrine, lagoonal and fluvio-deltaic paleoenvironments. An alkaline hypersaline lake, transitioning to sabkha, fluvial and lagoonal paleoenvironments was characterized by Salgado-Campos *et al.* (2022), who also proposed a regional arid to tropical climate humidification process, based on clay mineralogical data. Ramos *et al.* (2006) considered non-marine ostracod assemblages and the absence of marine microfossils to be indicative of lacustrine paleoenvironments.

Other paleontological findings, including fish remains (Lindoso *et al.* 2016), isopods (Lindoso *et al.* 2013), palynomorphs (Antonioli & Arai 2002) and ostracods associated with foraminifera and nannofossil (Barros *et al.* 2022; Santos *et al.* 2024), lead researchers to propose lagoonal and restricted lacustrine systems with marine influence. The possibility of marine ingressions was also suggested by geochemistry focused work (Bastos *et al.* 2014; Bastos *et al.* 2022; Rodrigues 1995; Sousa *et al.* 2019).

The Itapecuru Formation presents wide geographic distribution and approximately 600 m thickness in the Parnaíba Basin (Caputo 1984). It comprises sandstones, mudstones, siltstones, limestones, and palaeosols (Menezes *et al.* 2023; Rossetti *et al.* 2001; Vaz *et al.* 2007) which lie unconformably above the Grajaú and Codó formations (Góes & Feijó 1994; Vaz *et al.* 2007). Paleoenvironmental interpretations range from fluvial, estuarine and marginal marine environments (Caputo 1984; Corrêa-Martins *et al.* 2019; Lima *et al.* 1994; Rossetti *et al.* 2001). Palynological studies point to a tropical flora and warm climate (Arai 2001; Ferreira 2016; Pedrão *et al.* 1993; Pedrão 1995) influencing the deposition in floodplains during the upper Aptian (Ferreira *et al.* 2020) and Albian (Ferreira *et al.* 2016). Studies integrating ichnology and paleopedology proposed alluvial paleosols deposited under seasonal climate within the Equatorial Humid Belt (Menezes *et al.* 2019; 2023).

3 Material and Methods

3.1 Studied Material

The studied material originates from a 219.60 m thick interval (depths 14.40–234.00 m) sampled from the 2-CO-1-MA borehole. This section was drilled in July 2019 by the Alagoas Project. It is located 18 km southwest of Coroatá city, Maranhão State, northeastern Brazil (latitude 04°14′ 50.83″ S; longitude 44°14′26.24″ W), and reached a total depth of 251.20 m (Figure 2). The core is stored at the Laboratório de Geologia Sedimentar, Universidade Federal do Rio de Janeiro (Lagesed/UFRJ), Rio de Janeiro, Brazil. For this work, selected samples were subjected to analysis of calcareous microfossils, geochemistry and organic composition, and were statistically evaluated for the palynofacies analysis. Lithologic and facies descriptions of the rocks from which the analysed material was collected are available in Bobco *et al.* (2023).

3.2 Sample Preparation

For the analysis of ostracods, 63 samples, weighing 60 g each, were collected from lithologies that were favorable to the recovery these fossils, such as limestones, shales and other fine-grained sedimentary rocks. The average sample spacing was of approximately 3.5 m, with a regular interval of about 1 m maintained within shale sequences. In sandstone-dominated portions of the section, thin layers of clay and silt were sampled, resulting in a more irregular sampling interval (Figure 2). Calcareous microfossils were extracted using standard 'classic' procedures (Sohn 1961), which involved soaking the collected rock samples in 30% H_2O_2 for 4 h, followed by washing through a sieve set with mesh sizes of 250, 125 and 63 µm.

For the preparation of strew slides and kerogen concentrate mounts, 71 samples were collected from limestones, shales and other fine-grained sedimentary rocks. Standard non-oxidative procedures were used to isolate kerogen from the rock samples (Mendonça Filho *et al.* 2012; Oliveira *et al.* 2004; Tyson 1995). The samples were crushed until rock fragments approximately 2–5 mm in sizes. Acid treatment was conducted in three sequential steps, with neutralization of the solution between each step: first with 37 % HCl for 18 hours (to removal of carbonates), followed by 40% HF for 24h (to removal of silicates), and subsequently with 37% HCl for 3h (to eliminate newly formed fluorides). Finally, $ZnCl_2$ (with density of 1.9–2 g/cm^3) was use to kerogen concentration. The floated material was washed, and to eliminate any remaining heavy liquid, drops of 10% HCl and filtered water were added. The organic residue was then sieved using a 10 µm mesh. The Kerogen slides are archived at the Laboratório de Palinofácies e Fácies Orgânica (LAFO), Universidade Federal do Rio de Janeiro (UFRJ), Rio de Janeiro, Brazil.

3.3 Geochemical Analysis

The quantification of Total Organic Carbon (TOC) and Total Sulfur (TS) levels in the samples was carried out after acidification to eliminate carbonates, employing a LECO SC 144 analyzer, in accordance with the ASTM Standard D4239-08 (2008). The Insoluble Residue (IR) represents the fraction of the sample that remains after acidification.

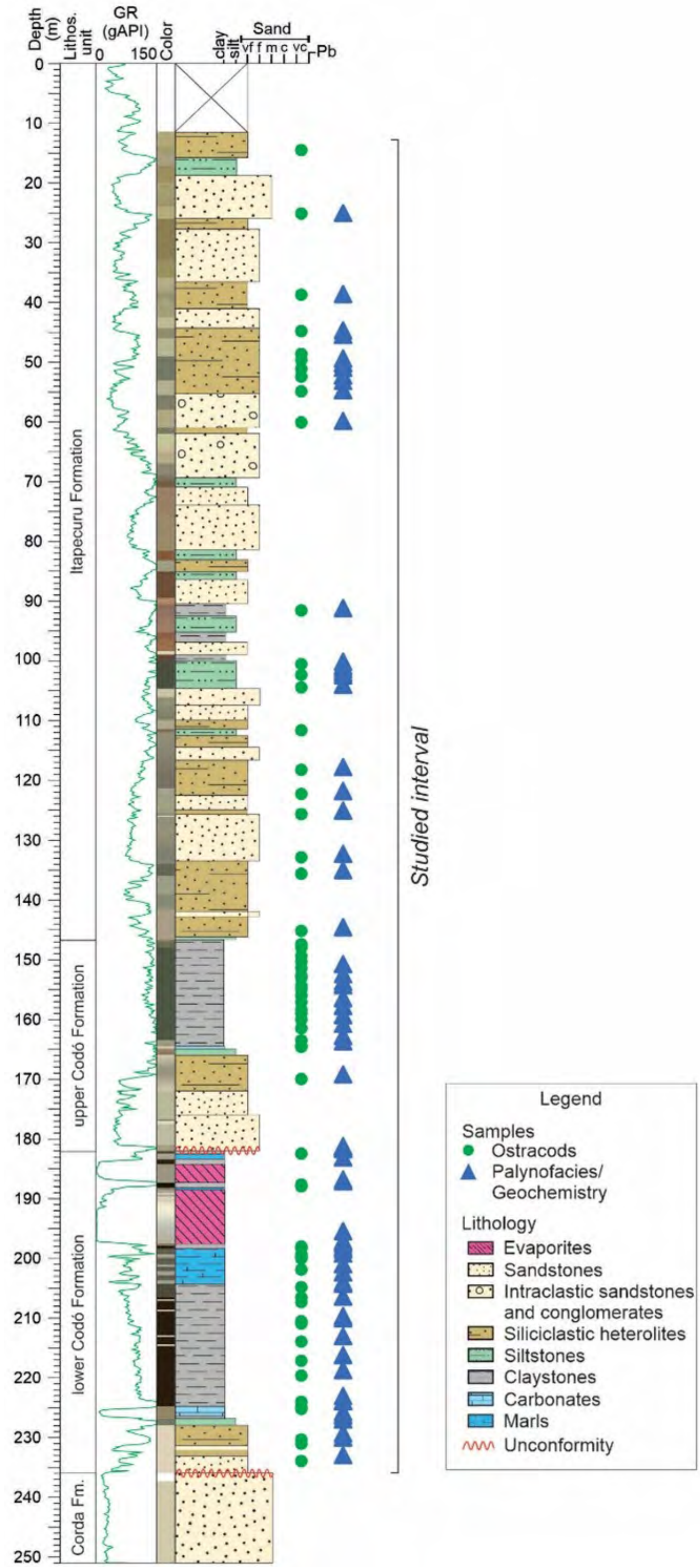

Figure 2 Lithological description, gamma-ray log (GR) and lithostratigraphic units of the 2-CO-1-MA borehole (adapted from Bobco *et al.* 2023), with indication of samples and interval studied in this work

CC BY

3.4 Calcareous Microfossil Analysis

Picking of ostracods and other fossil material was conducted on sediment fractions retained in 250 µm, 125 µm and 63 µm mesh sieves, using a Leica M165C stereomicroscope at magnification ranging from 7.3X to 120X. A minimum of 300 specimens per sample is considered ideal for the statistical representation of a population (Dennison & Hay 1967; Fatela & Taborda 2002). Accordingly, samples containing less than 300 specimens (which applied to all but three samples) were completely picked, whereas samples with significantly higher number of specimens (224.10 m; 224.90 m and 225.30 m) were split into subsamples until a fraction yielding approximately 300 specimens was obtained (1/32; ¼ and ½, respectively). Total abundance was then calculated based on the analysed fraction (see Supplementary Material). Adult and juvenile carapaces, valves and molds were each counted as a specimen.

Ostracod specimens were identified following specialized literature (Antonietto 2010; Bate 1972; Bate *et al.* 2022; Coimbra *et al.* 2002; Do Carmo *et al.* 2008; 2013; Guzmán *et al.* 2022; Krömmelbein & Weber 1971; Melo *et al.* 2020; Ramos *et al.* 2006; Tomé *et al.* 2014). Suprageneric classification followed the scheme proposed by Horne (2005). Total abundance of ostracods and other fossil material was obtained for each sample. To support the paleoecological analysis, relative abundance and Shannon-Wiener diversity index were calculated using PAST ® software (Hammer *et al.* 2001). Figures and plots were generated using PanPlot 2 (Sieger & Grobe 2013) and CorelDRAW® software.

Scanning electron microscope images (SEM) of the specimens were obtained at the Centro de Tecnologia Mineral/Ministério da Ciência, Tecnologia e Inovação (CETEM/MCTI), Rio de Janeiro, Brazil using a HITACHI 3030TM Plus equipment operating at 15 kV in a low vacuum mode and using a secondary electron detector. The specimens are curated at the Laboratório de Micropaleontologia Aplicada, Universidade Federal do Rio de Janeiro (MicrA/UFRJ), Rio de Janeiro, Brazil, under catalog codes LM-21/001–LM-21/052 and LM-21/308–LM-21/319.

3.5 Organic Composition Analysis, Statistical Treatment and Palynofacies

The analysis involved the qualitative identification of organic particle components, classified into groups and subgroups, using microscopic techniques under both transmitted white light (TWL) and incident blue light fluorescence microscopy (FM). Quantitative examination was also performed by counting 300 to 500 particles, following the organic matter groups and subgroups classification proposed by Tyson (1995), and updated by Mendonça Filho & Gonçalves (2017) and Mendonça Filho *et al.* (2010, 2012, 2017).

A statistical analysis of the organic matter components counted in the studied samples was performed (see Supplementary Material). Data were recalculated and normalized to percentages values. Cluster analysis was used to evaluate the degree of similarity among groups and subgroups of organic matter components, grouping them into sets with higher similarity. Q-mode clustering analysis was used to determine similarities between samples, whereas R-mode clustering was performed to verify similarities among kerogen groups and subgroups, based on correlation coefficient Pearson. Statistical treatment was carried out using StatSoft® STATISTICA software, version 7.0 (Valentin 2000).

4 Results

4.1 Micropaleontology

4.1.1. Ostracods

Four ostracod species, belonging to two genera and two families, were identified in the analysed samples. The most representative ostracod specimens are illustrated in Figure 3 and detailed taxonomic notes are available in the Appendix. Among 2,864 ostracod specimens picked, 872 (30.45%) are representatives of the Family Candonidae, genus *Damonella*, and 265 (9.25%) belong to the Family Cyprididae, genus *Pattersoncypris*; the remaining specimens (60.30%) were very poorly preserved and recorded as indeterminate ostracods. The predominant taxon is *Damonella grandiensis* (24.65%), followed by *Pattersoncypris micropapillosa* (3.63%), *Pattersoncypris symmetrica* (1.78%), and *Pattersoncypris* sp. (0.28%). Some specimens were identified only at the generic level, as their state of preservation did not permit assignment to specific species. These were registered as *Damonella* spp. (5.80%) and *Pattersoncypris* spp. (3.56%).

4.1.2. Associated Fossil Material

In addition to ostracods, other fossil material recovered from the analysed samples include megaspores, *Microcarpolithes hexagonalis* Vangerow, 1954 (interpreted as termite coprolites, see Colin *et al.* 2011), Gastropoda, fish fragments, and foraminifera. The most representative examples of this associated fossil material are illustrated in Figure 4.

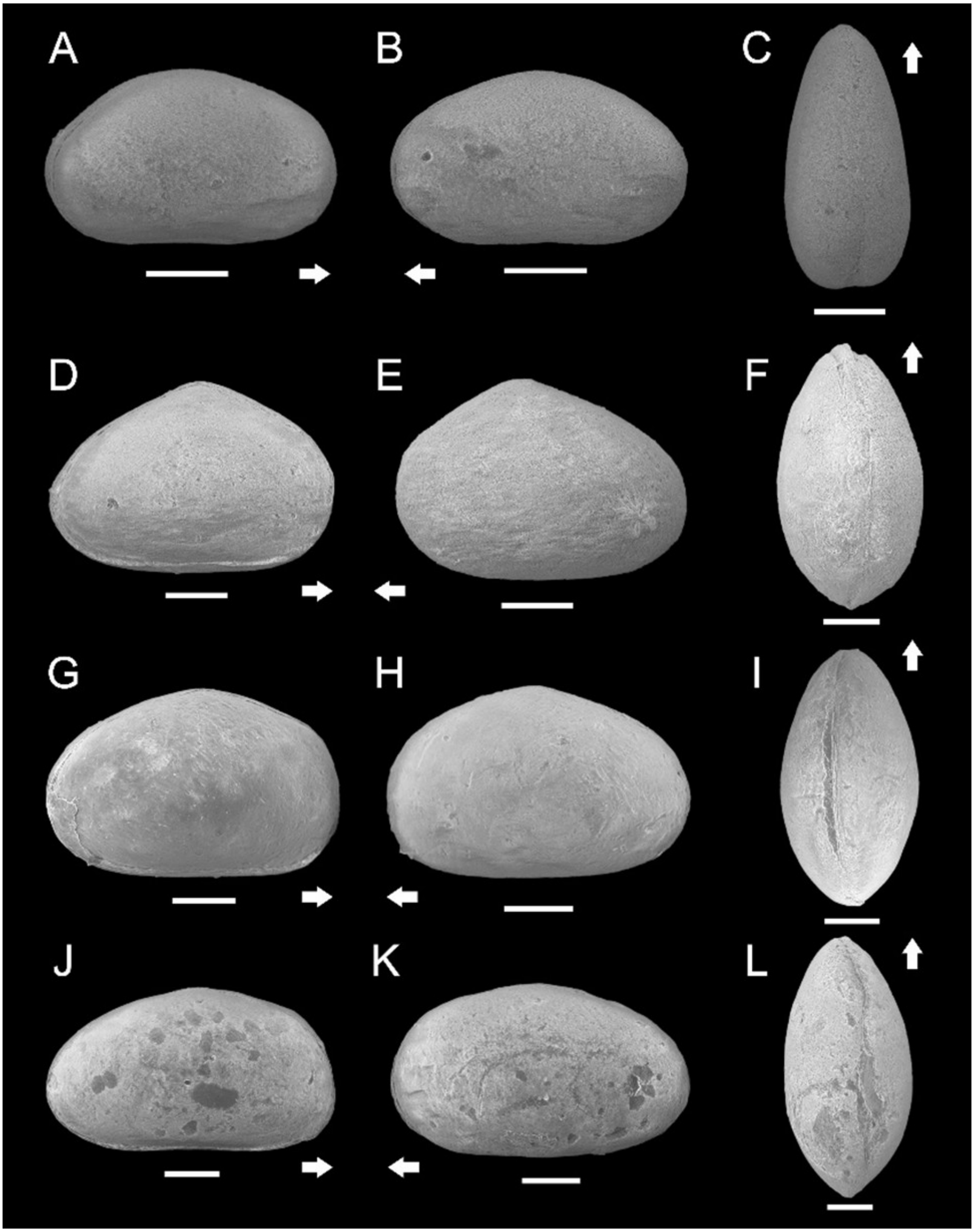

Figure 3 Ostracod species identified in this study. Scale = 200 µm: A–C: *Damonella grandiensis* Tomé *et al.* 2014; A: LM-21/023A, depth of 151.40 m, RV, L: 714 µm, H: 425 µm; B: LM-21/023B, depth of 151.40 m, LV, L: 719 µm, H: 420 µm; C: LM-21/023C, depth of 151.40 m, DV, W: 360 µm; D–F. *Pattersoncypris micropapillosa* Bate, 1972. D. LM-21/023D, depth of 151.40 m, RV, L: 928 µm, H: 623 µm; E. LM-21/310A, depth of 150.40 m, LV, L: 810 µm, H: 563 µm; F. LM-21/310B, depth of 150.40 m, DV, W: 519 µm; G–I: *Pattersoncypris symmetrica* (Krömmelbein & Weber 1971); G. LM-21/313A, depth of 159.00 m, RV, L: 929 µm, H: 596 µm; H: LM-21/313B, depth of 159.00 m, LV, L: 883 µm, H: 558 µm; I. LM-21/313C, depth of 159.00 m, DV, W: 511 µm; J–L. *Pattersoncypris* sp.. J. LM-21/027A, depth of 157.10 m, RV, L. 1067 µm, H: 599 µm; K: LM-21/027B, depth of 157.10 m, LV, L: 1030 µm, H: 599 µm; L. LM-21/027C, depth of 157.10 m, DV, W: 570 µm.

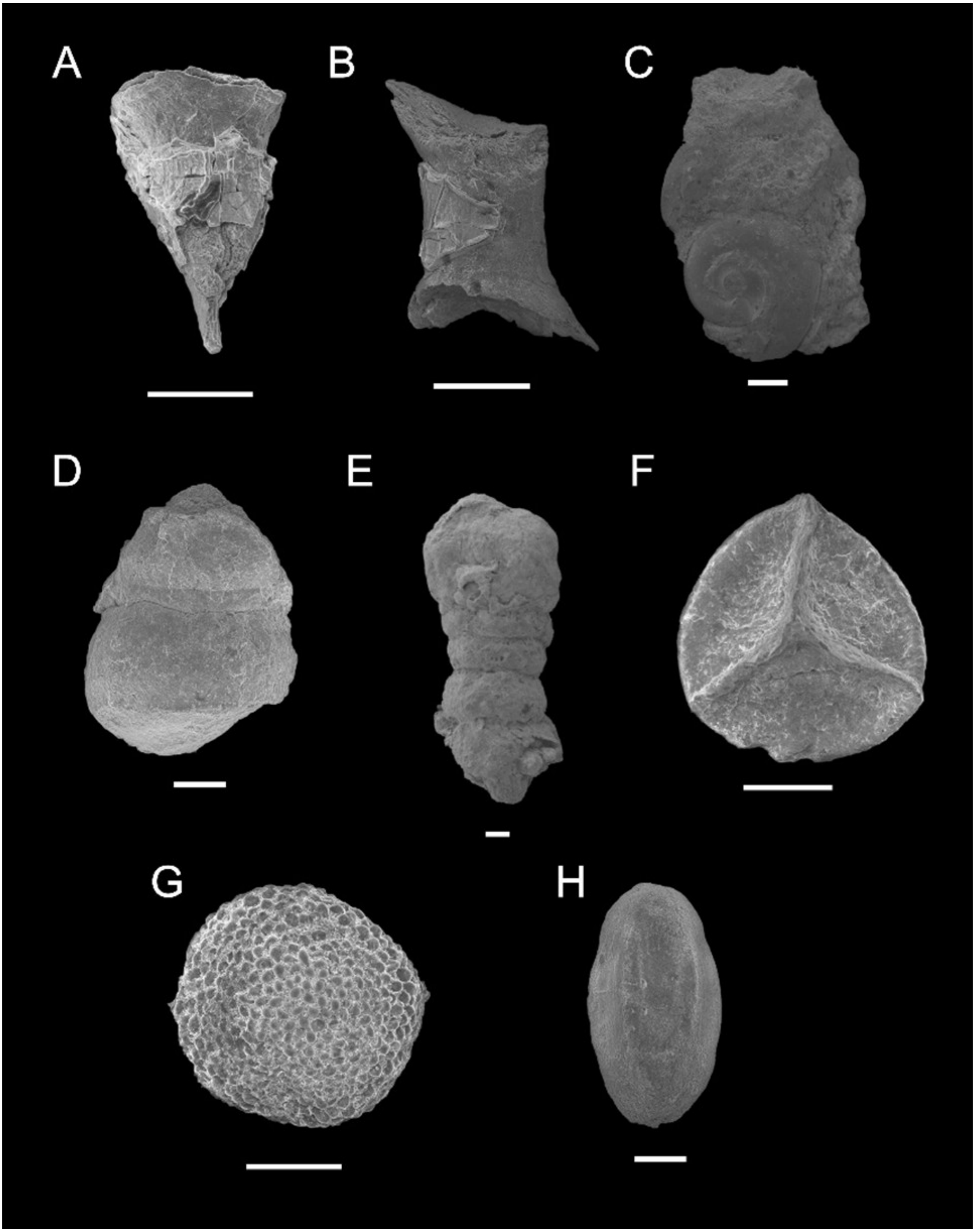

Figure 4 Associated fossil material: A. Fish teeth, LM-21/022A, depth of 148,00; B. Fish vertebrae, LM-21/022B, depth of 148,00; C. Gastropoda, LM-21/319A, depth of 225,30; D. Gastropoda, LM-21/309A, depth of 149,40; E. Foraminifera indet., LM-21/034A, depth of 182,50; F. Megaspore, LM-21/006A, depth of 51,00; G. Megaspore, LM-21/011A, depth of 100,50; H. *Microcarpolithes hexagonalis* Vangerow, 1954 (termite coprolite), LM-21/006B, depth of 51,00. Scale = 200 µm.

4.1.3. Microfossil Associations

Based on variations in the relative abundance of ostracod taxa and total abundance of all fossil groups throughout the studied well, the samples were grouped into four microfossil associations (MA-1, MA-2, MA-3 and MA-4), as illustrated in Figures 5 and 6.

Microfossil association MA-1 is characterized by the presence of megaspores associated with the termite coprolite *Microcarpolithes hexagonalis*, gastropods and fish fragments. Ostracods are exceedingly rare within this association and, when present, are poorly preserved, often exhibiting signs of fragmentation, oxidation, and dissolution; consequently, they have been registered as indeterminate ostracods. This microfossil association characterizes the intervals between 240 to 227 m, from 146 to 90 m and from 62 to 50 m.

Microfossil association MA-2 is similarly characterized by the presence of *M. hexagonalis*, gastropods and fish fragments, but also presents poorly preserved, abundant ostracod assemblages. Juvenile forms predominate, with adult ostracods notably absent. Some specimens exhibit pyritization and recrystallization. This association is recorded in samples from depths of 225.30, 224.60 and 224.10 m, all of which contain a very high abundance of degraded ostracod shells, predominantly represented by disarticulated juvenile molds and casts. In these samples, identification was possible to the generic level for certain specimens, while others were registered as indeterminate ostracods.

Microfossil association MA-3 is defined by moderately abundant, poorly preserved ostracod assemblages, with specimens showing intense recrystallization and thus classified as indeterminate. Juvenile ostracods with closed carapaces, often affected by pyritization, are also observed. Additionally, agglutinated benthic foraminifera were identified in sample 182.50 m. This association occurs between depths of 208 m and 181 m.

Microfossil association MA-4 is characterized by moderately abundant ostracod assemblages, with counts ranging from approximately 50 to 200 specimens per sample. The ostracods are moderate to poorly preserved, predominantly occurring articulated juvenile carapaces, while adult specimens are rare. Many individuals present recrystallization and pyritization, which prevented identification at the specific and, some cases, even the generic level. Consequently, these specimens were classified as *Pattersoncypris* spp., *Damonella* spp. and indeterminate ostracods (Ostrac. Indet.). *Damonella grandiensis* is the dominant species across most samples, associated with *Pattersoncypris micropapillosa*, *Pattersoncypris symmetrica* and *Pattersoncypris* sp. This microfossil association is characteristic of the interval between 166 to 146 m. For this interval, the Shannon Diversity Index was calculated, yielding values ranging from 0 to 0.6931, with an average of 0.327.

4.2 Geochemistry

The studied samples show TOC values ranging from 0.14 to 19.60 wt.%, average of 2.06 wt.%. TS values range from 0.01 to 25.01 wt.%, averaging 1.38 wt.%. IR values vary between 27 to 93 wt.%, with an average of 77 wt.%. The results for TOC, TS and IR are illustrated in Figure 7.

4.3 Organic Compostion

The analysis identified organic components representing all three main groups of particulate organic matter, as defined by Tyson (1995) and later updated by Mendonça Filho & Gonçalves (2017): Phytoclast, Amorphous and Palynomorph (Figure 7). Representative examples of each group are illustrated in Figure 8.

The Phytoclast group display values of up to 95.24 wt.% (44.53 wt.% average). This group is represented by degraded non-opaque phytoclasts (13.34 wt.% average), non-degraded non-opaque phytoclasts, opaque phytoclasts, as well as cuticles and membranes.

The Amorphous group occurs with values of up to 0.00 to 99.36 wt.% (38.07 wt.% average). This group is subdivided into terrestrially derived amorphous organic matter (Terrestrially Derived AOM), ranging from 0.00 to 74.92 wt.%, (20.50 wt.% average) and bacterial amorphous organic matter (Bacterial AOM), ranging from 0.00 to 99.36 wt.% (16.80 wt.% average).

The Palynomorph group ranges from 0.00 to 55.13 wt.% (average 17.40 wt.%) and is predominantly composed of sporomorphs (average 11.92 wt.%), including spores and pollen grains. Spores vary in size, shape (oval to triangular), and exhibit trilete or monolete marks, with colors from pale yellow to black in TWL and fluorescence from dark yellow to brown. Pollen grains display diverse ornamentation, morphology, and coloration under both transmitted and incident blue light. Freshwater microplankton (average 0.76 wt.%), represented by *Pediastrum*, *Botryococcus*, *Zygnemataceae*, and *Scenedesmus* genera, and marine microplankton (0.00–7.76 wt.%, average 0.36 wt.%), mainly dinoflagellate cysts (*Subtilisphaera* genus), are also present.

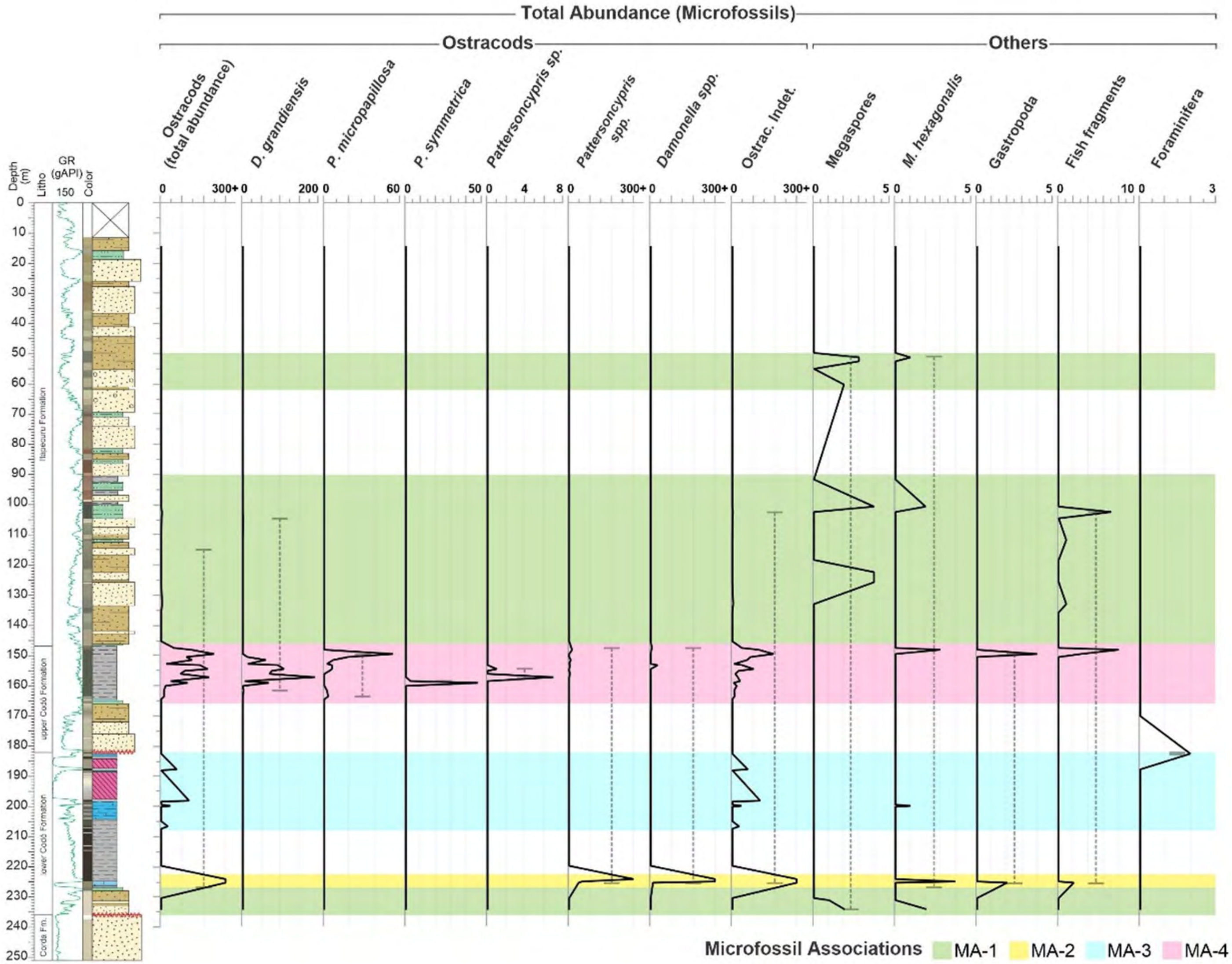

Figure 5 Total abundance of all retrieved taxa along the studied section. Microfossil associations (MA-1, MA-2, MA-3 and MA-4) are colored in green, yellow, blue and pink, respectively. Gamma-ray log (GR) is colored in green.

CC BY

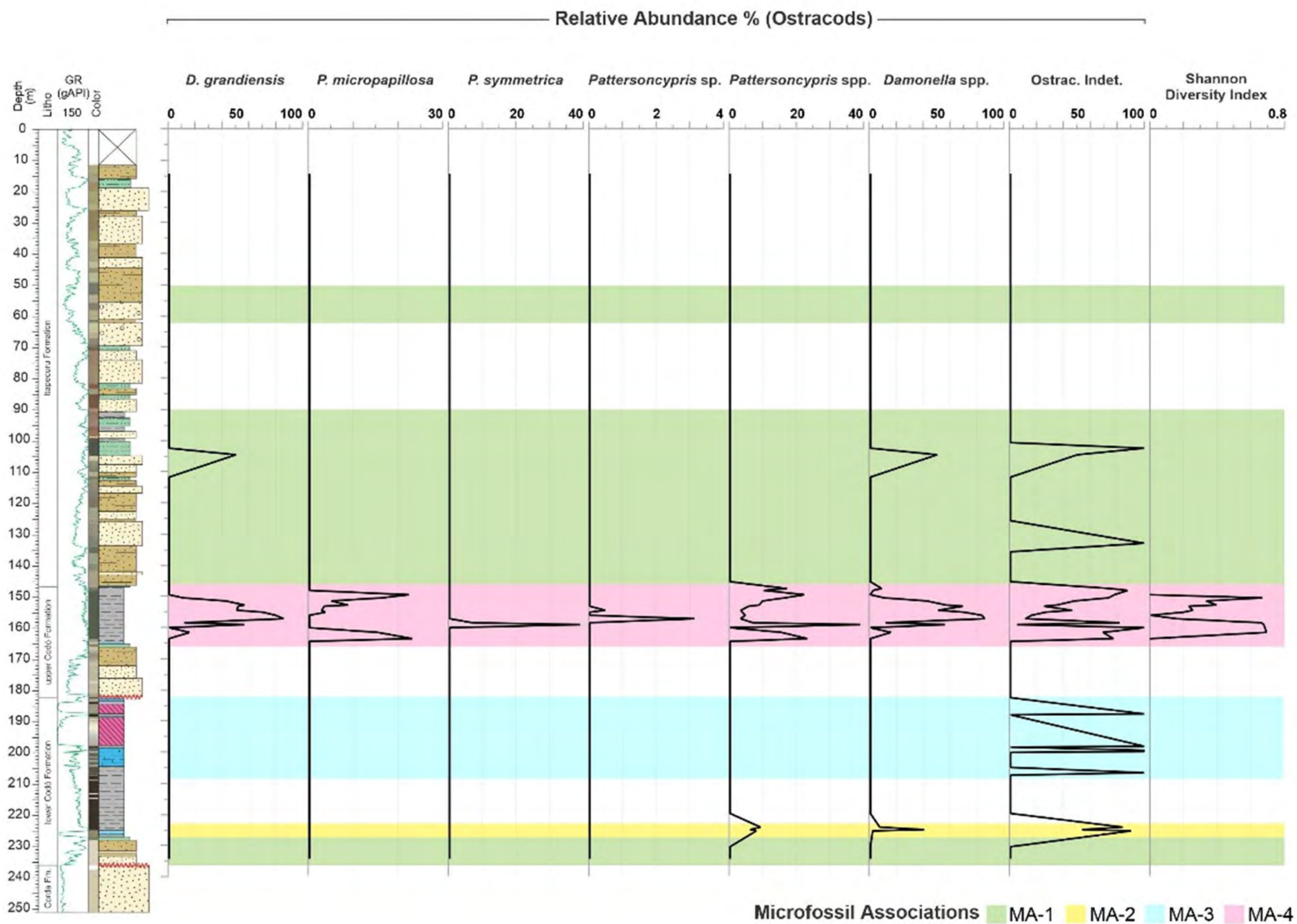

Figure 6 Relative abundance of ostracods along the studied section. Microfossil associations (MA-1, MA-2, MA-3 and MA-4) are colored in green, yellow, blue and pink, respectively. Shannon Diversity Index obtained for microfossil association MA-4. Gamma-ray log (GR) is colored in green.

CC BY

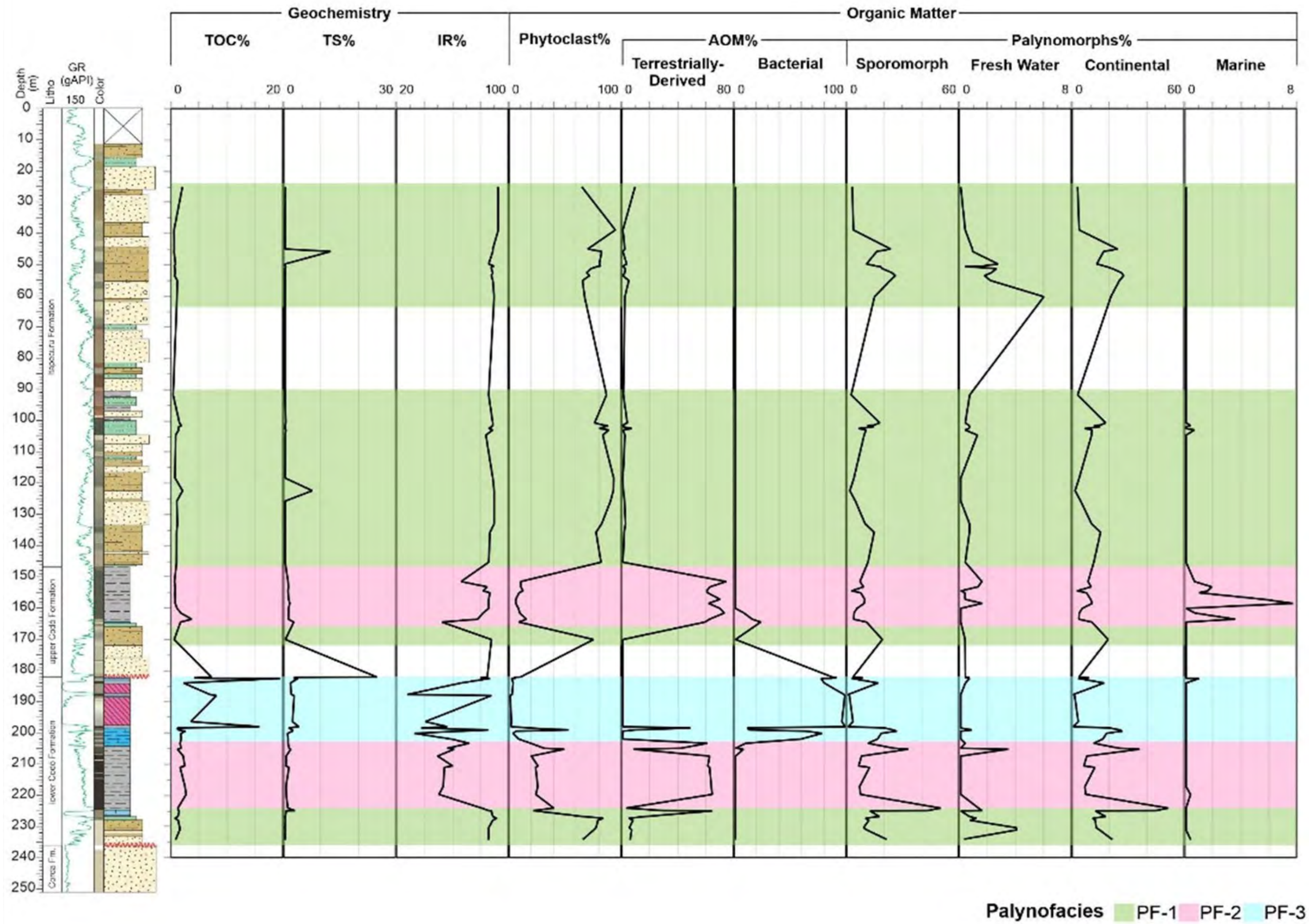

Figure 7 Geochemistry and Palynofacies results plotted against the studied section. Palynofacies (PF-1, PF-2 and PF-3) are colored in green, pink and blue, respectively. Gamma-ray log (GR) is colored in green.

CC BY

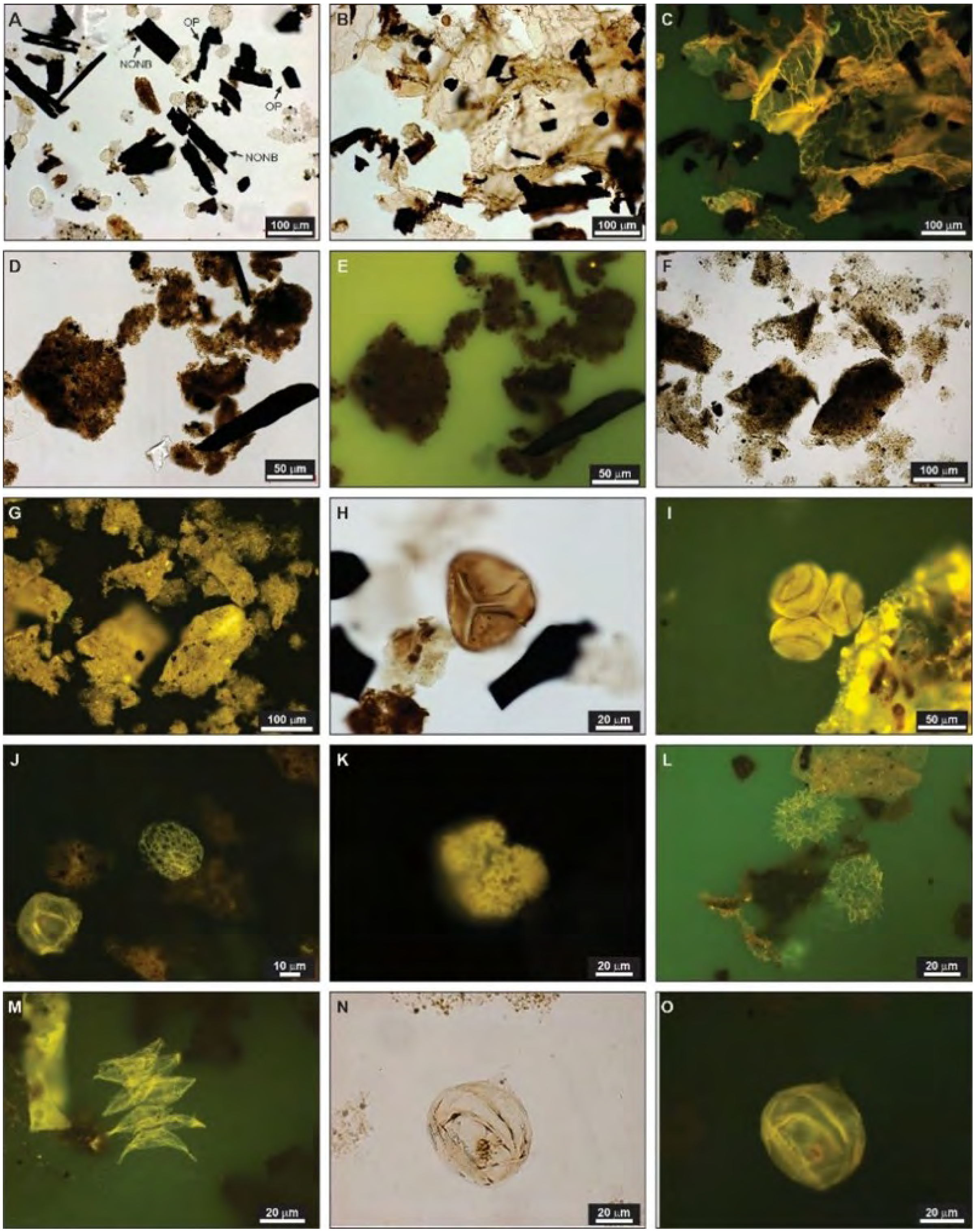

Figure 8 Photomicrographs of the organic components belonging to the Phytoclast, Amorphous and Palynomorph groups identified in the studied samples: A. Opaque phytoclasts and Non-opaque phytoclasts (depth of 205.20 m); B-C. Membrane (depth of 227.35 m); D-E. Terrestrially-derived AOM (depth of 207.40 m); E, F and G. Plate-like bacterial-derived AOM (depth of 182.05 m); H. Trilete spores (depth of 224.10 m); I. Tetrad of pollen grains, *Classopollis* genus (depth of 224.10 m); J. *Afropollis* genus (depth of 198.40 m); K. *Botryococcus* sp. (depth of 224.10 m); L. *Pediastrum* sp. (depth of 230.40 m); M. *Scenedesmus* sp. (depth of 231.10 m); N-O. Dinoflagellate cysts (*Subtilisphaera* spp.), (depth of 157.10 m). TWL: A, B, D, F, H and N; FM: C, E, G, I–M and O.

4.4 Palynofacies

Cluster analysis was applied using both compositional data (R-mode) and percentage distributions (Q-mode) of kerogen components to establish groupings and explore the relationships between them. The R-mode analysis enabled the classification of organic matter components into three distinct groups (A, B, and C), reflecting their degree of similarity and origin. Group A, which is characterized by components belonging to the Phytoclast Group (non-opaque phytoclast, opaque phytoclast and cuticle/membranes), along with elements of Sporomorph subgroup (spores and pollen grains) and the Freshwater Microplankton subgroup. Group B is characterized by the predominance of terrestrially derived amorphous organic matter (Terrestrially Derived AOM), while Group C is characterized by the association of bacterial amorphous organic matter (Bacterial AOM), Total Organic Carbon (TOC), and Total Sulphur (TS) and low marine influence in the form of dinoflagellate cysts (see Supplementary Material).

Based on the abundance patterns of kerogen groups and subgroups, the Q-Mode cluster analysis further allowed the identification of three distinct palynofacies (Figure 7):

Palynofacies PF-1 is characterized by the lowest average contents of TOC and TS, measuring 0.86 wt.% and 0.79 wt.%, respectively. In contrast, it presents the highest average contents of IR, at 87.41 wt.%. This palynofacies is dominated by components of the Phytoclast Group, which reach up to 95.24 wt.%, with an average of 75.32 wt.%. Within this group, non-opaque phytoclasts predominate, averaging 40.45 wt.%, of which degraded non-opaque phytoclasts account for an average of 20.23 wt.%. These are followed by opaque phytoclasts (average of 22.07 wt.%) and cuticles and membranes (average of 12.79 wt.%). Palynomorphs are also present, reaching up to 55.13 wt% (average of 19.37 wt%). This subgroup is dominated by sporomorphs (spores and pollen grains), which can reach up to 50.32 wt% and average 15.15 wt%. Freshwater microplankton are recorded throughout the sequence with an average of 1.24 wt%, while marine microplankton, represented by dinoflagellate cysts, occur with an average of 0.04 wt%. These marine forms were observed in samples collected at 234.00, 219.70, 102.75, 101.35, and 101.20 m. The Amorphous Group occurs in percentage of up to 31.38 wt.% (average of 5.31 wt.%), predominantly comprising terrestrially derived amorphous organic matter (Terrestrially Derived AOM), which reaches up to 29.23 wt% (average of 3.51 wt%). This is followed by bacterial amorphous organic matter (Bacterial AOM), which reaches up to 12.33 wt%, with an average of 0.53 wt%.

Palynofacies PF-2 presents TOC contents between 0.40 and 3.52 wt.% (average of 1.45 wt.%), TS contents between 0.28 and 2.38 wt.% (average of 0.84 wt.%) and IR with an average of 66.90 wt.%. The Amorphous Group predominates in this palynofacies, with percentage values ranging from 42.00 to 82.32 wt% and an average of 66.24 wt%. It is dominated by Terrestrially-Derived AOM, reaching up to 74.82 wt.% and averaging 63.20 wt%. Bacterial AOM is less abundant, with values between 0.00 and 22.83 wt% (average of 3.12 wt%). The Palynomorph Group occurs with percentages reaching up to 32.92 wt.% (average of 18.01 wt.%), represented by continental palynomorphs, particularly sporomorph subgroup (spores and pollen grains), which range from 1.87 to 25.00 wt% and average 8.66 wt%. Freshwater microplankton are present in some samples from the middle and upper portions of the studied section, with an average of 0.25 wt%. Marine microplankton, represented by dinoflagellate cysts, were identified in samples from depths of 219.70, 163.50, 161.50, 158.40, 157.10, 155.00, 154.40, 153.10, and 151.40 m. The highest value recorded was 7.76 wt% at 158.40 m, with an average of 1.09 wt% across this palynofacies. Phytoclast Group components occur in proportion ranging from 4.97 and 30.67 wt.% (average of 15.75 wt.%). These are primarily represented by non-opaque phytoclasts, with an average of 12.88 wt.% (of which non-opaque non-degraded phytoclast account for 9.32 wt.%), followed by opaque phytoclasts, which average 2.73 wt.%.

Palynofacies PF-3 is characterized by the highest TOC values among the identified palynofacies, ranging from 1.57 to 19.60 wt.% (average of 6.49 wt.%). TS contents also reach elevated levels, varying between 0.71 and 25.01 wt% (average of 3.95 wt%). In contrast, Insoluble Residue (IR) values are the lowest recorded, ranging from 27.00 to 88.00 wt%, with an average of 65.92 wt%. The Amorphous Group predominates, particularly bacterial amorphous organic matter (Bacterial AOM), which reaches up to 99.36 wt% and averages 85.20 wt%. Palynomorphs are also present, with an average of 10.79 wt%, primarily represented by sporomorphs (spores and pollen grains), which account for an average of 7.97 wt%. Freshwater microplankton were identified at the top of the section, albeit in minor amounts, averaging 0.22 wt%. Marine microplankton, represented by dinoflagellate cysts, were recorded only in sample 182.50 m, where they represent 0.95 wt% of that sample and average just 0.07 wt% across the entire palynofacies.

5 Discussion

5.1 Biostratigraphic Framework

The identification of *Damonella grandiensis* and *Pattersoncypris micropapillosa* in the samples allows correlation with the *Cytheridea*? spp. 201–218 Biozone,

CC BY

code 011 (Moura 1988; hereby referred to as Biozone 011). This biostratigraphic unit was informally proposed in the Sergipe-Alagoas Basin, based on the occurrence of of several ostracod species, including the unillustrated “Ostracod 207” (Schaller 1969). Later, Moura (1988) formally recognized this zone in the Campos Basin, describing it as a “poor ostracod assemblage in which only some components are recognizable”, and provided illustration of selected species. Subsequently, Coimbra *et al.* (2002) identified Biozone 011 it in the Araripe Basin. Although no definitive index species were found, the persistent and abundant presence of Ostracod sp. 207 led them to assign the sequence to the *Cytheridea*? spp. 201–218 Zone (NRT-011). In a significant taxonomic revision, Do Carmo *et al.* (2008) proposed synonymizing of five *Pattersoncypris* species with the Chinese genus *Harbinia*, identifying *Pattersoncypris micropapillosa* (referred to as *Harbinia micropapillosa* by the author) as the index species for Biozone 011. Other *Pattersoncypris* species were considered additional markers of this unit. This taxonomic approach, however, was later challenged by Poropat and Colin (2012b), who rejected the synonymies but agreed with Do Carmo *et al.* (2008) regarding the use of *Pattersoncypris micropapillosa* to typify the biozone. Further refinement was made by Tomé *et al.* (2014), who described *Damonella grandiensis* and proposed its conspecificity with the previously informal “Ostracod 207”. Later, Nascimento *et al.* (2017) recommended redefining Biozone 011 as an “occurrence zone”, based on the presence of *Damonella grandiensis* as an index species. More recently, Guzmán *et al.* (2023) reviewed this biostratigraphic unit, renaming it as *Pattersoncypris micropapillosa* (OST-011) Biozone and proposing its classification as a taxon-range zone, with *Pattersoncypris micropapillosa* designated as the index species. Additionally, they subdivided the unit into four subzones, including the *Damonella grandiensis* Assemblage Subzone (OST-011.3), whose lower and upper boundaries are defined by the first local lowest occurrences of *Neuquenocypris berthoui* and *Pattersoncypris kroemmelbeini*, respectively.

In this work, the occurrences of *Damonella grandiensis* and *Pattersoncypris micropapillosa* were used to define the Biozone 011. The local lowest occurrences of *Pattersoncypris* spp. and *Damonella* spp. at a depth of 225.30 m were used to establish the provisional lower boundary of the zone. However, due to the poor preservation of specimens in the lower part of the studied interval, which restricted identification to the generic level, this limit is regarded with a degree of uncertainty. A more reliable lower boundary was determined based on the local lowest occurrence of *Pattersoncypris micropapillosa* at 163.50 m, where improved preservation enabled confident identification at the species level. The upper boundary of Biozone 011 was defined by the local highest occurrence of *Damonella grandiensis* at a depth of 104.40 m (Figure 9)

This biozone is assigned to the Alagoas local Stage, which is commonly correlated with the upper Aptian–Albian (Do Carmo *et al.* 2008; Moura 1988; Nascimento *et al.* 2017; Poropat & Colin, 2012a; Schaller 1969). However, this correlation has been questioned by some authors, primarily due to the lack of global chronostratigraphic markers (Antunes *et al.* 2018; Lúcio *et al.* 2020). Despite these uncertainties the robustness of the Lower Cretaceous biostratigraphic framework across the northeastern Brazilian basins has been highlighted by Coimbra & Freire (2021), and further reinforced by recent studies that calibrated these biozones with foraminifera record (Araripe *et al.* 2022; Guzmán *et al.* 2023; Melo *et al.* 2020).

Guzmán *et al.* (2023) define the *Damonella grandiensis* (OST-011.3) subzone, which is characterized by a conspicuous abundance of *Damonella grandiensis* and *Pattersoncypris micropapillosa*. According to their zonation, the OST-011.3 subzone is positioned stratigraphically between the *P. cucurves–N. berthoui* OST-011.2 subzone, correlated to the planktic foraminifera *Leopoldina*? *cabri* zone, and the *P. crepata* OST-011.4 subzone, which is linked to the *Hedbergella infracretacea–Microhedbergella miniglobularis* composite zone, placing OST-011.3 within the Aptian to upper Aptian. The ostracod assemblages documented in this study exhibit similarities with the OST-011.3 subzone, exhibiting moderately abundant *Damonella grandiensis* and *Pattersoncypris micropapillosa* assemblages. Nevertheless, these assemblages show lower diversity and poorer preservation when compared to those previously described. Furthermore, it is important to note that *N. berthoui*, the ostracod used by Guzmán *et al.* (2023) to define the lower boundary of OST-011.3, was not recorded in the 2-CO-1-MA section. The local lowest occurrence of *Pattersoncypris symmetrica*, used in conjunction with *P. kroemmelbeini* to mark the upper boundary of OST-011.3, was registered at a depth of 159.00 m in the 2-CO-1-MA section. This observation suggests that Biozone 011 in the upper Codó Formation may be situated near the transition between the OST-011.3 and OST-011.4 subzones, which is correlated with the upper Aptian.

In addition to the ostracods, the occurrence of *Sergipea variverrucata* was registered at a depth 101.75 m in the 2-CO-1-MA well (Guerra-Sommer *et al.* 2021). This palynomorph is widely regarded by several authors as being restricted to the upper Aptian (Arai & Assine, 2020; Arai *et al.* 1989; Coimbra & Freire, 2021; Ferreira *et al.* 2020; Regali & Viana 1989; Rios-Netto *et al.* 2012; Rossetti *et al.* 2001).

CC BY

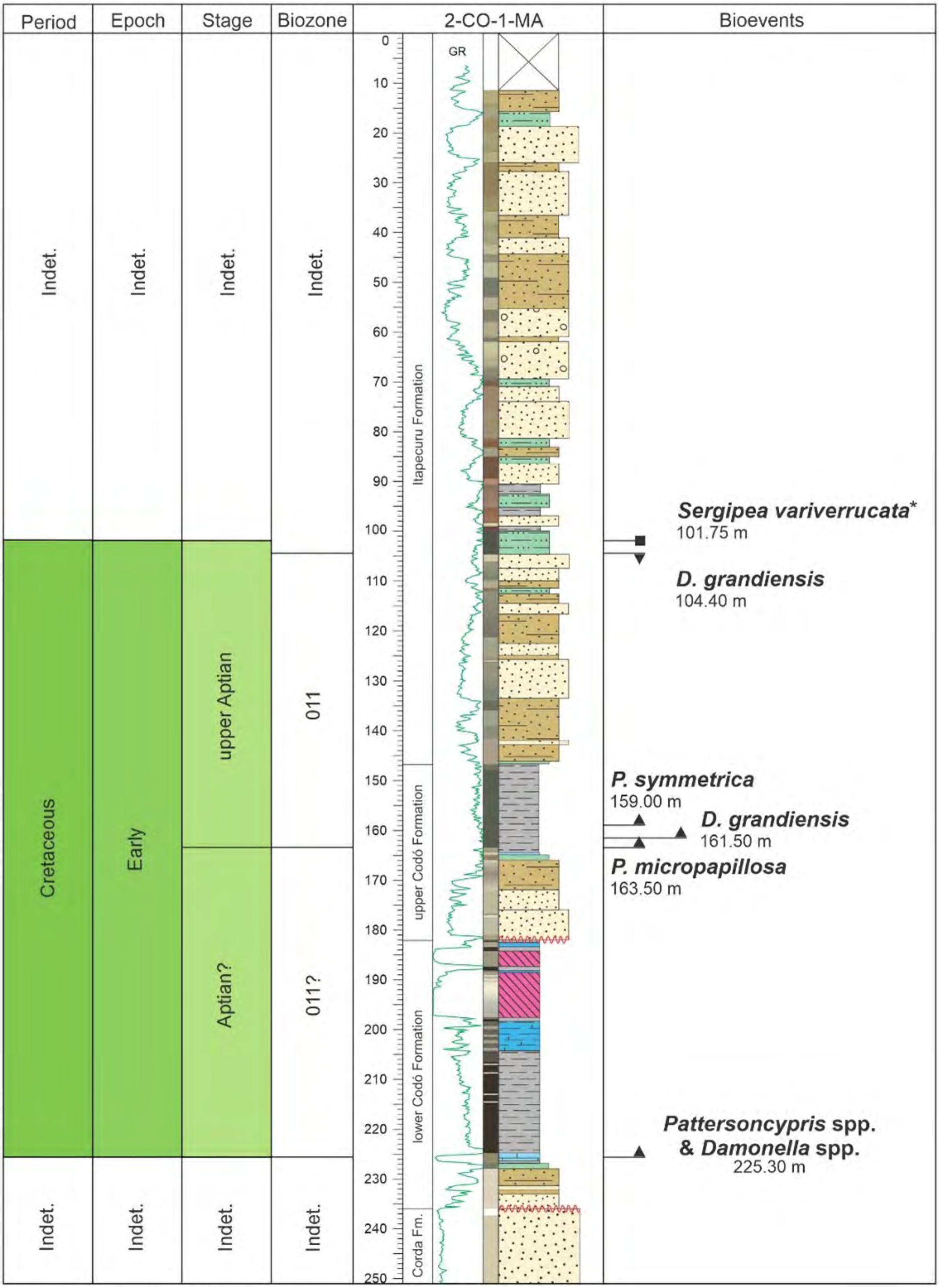

Figure 9 Biostratigraphic framework of the 2-CO-1-MA well. * The presence of the palynomorph *Sergipea variverrucata* was recorded at 101.75 m by Guerra-Sommer *et al.* 2021. Gamma-ray log (GR) is colored in green.

CC BY

Based on the integration of this palynological evidence with the ostracod data, the interval between 163.50 m and 101.75 m in the studied section was assigned to the upper Aptian. However, the intervals below 225.30 m and above 101.75 m (up to 14.40 m depth) remain indeterminate, as they were either barren or yielded only rare, poorly preserved ostracods that could not be reliably identified.

5.2 Paleoenvironments

Based on the microfossil associations (MA-1, MA-2, MA-3 and MA-4) and palynofacies (PF-1, PF-2 and PF-3) described in section 4, six paleoenvironmental intervals are proposed for the 2-CO-1-MA section. The depositional stages proposed by Bobco *et al.* (2023) were also used to evaluate and propose PI-1 to PI-3. The paleoenvironmental intervals (PI-1 to PI-6) are summarized and illustrated in Figure 10.

PI-1 (236 to 227 m) is characterized in our work by MA-1, represented by *Microcarpolithes hexagonalis* and megaspores. The palynofacies PF-1 is dominated by components of terrestrial continental organic matter, mainly phytoclasts (wood, cuticles and membranes) and sporomorphs (spores and pollen grains), with high IR wt%. This is consistent with a freshwater environment, with oxic regime, strongly influenced by higher terrestrial plants and with incipient marine influence (0.34 wt.% of *Subtilisphaera* spp. dinoflagellate cysts in sample 234.00 m). The presence of *M. hexagonalis* possibly indicates low-energy, stable environments, such as floodplains, lacustrine margins, soils, or swampy areas with high organic productivity (Colin *et al.* 2011; Mcloughlin *et al.* 2024, Ősi *et al.*, 2021; Pires & Sommer 2009). This interval was interpreted by Bobco *et al.* (2023) as an expanded lake system with high continental humidity, highlighting sedimentary facies which were consistent with abundant terrigenous sedimentary input and organic matter. The occurrence of an ichnofabric indicative of marine influence (*Diplocraterion*) was also noted in that work, supporting incipient marine influence. Hence, a lacustrine paleoenvironment, with low marine influence, can be interpreted for PI-1.

PI-2 (227 to 203 m) includes MA-2, which occurs at discrete levels in the base of the interval (samples 225.30 m, 224.60 m and 224.10 m) and is characterized by abundant ostracod assemblages composed by disarticulated juvenile specimens. Juvenile disarticulated valves of *Damonella* spp., *Pattersoncypris* spp., and indeterminate ostracods are present, exhibiting signs of pyritization, possibly evidencing episodes with anoxic conditions (Boomer & Eisenhauer, 2002; Boomer *et al.* 2003; Carbonel *et al.* 1988; Neale 1988). The rest of the interval is almost devoid of ostracods, with sample 206.60 m representing intensely recrystallized indeterminate specimens. The palynofacies PF-2 is dominated by Terrestrially-Derived AOM, which indicates stagnant water bodies with reducing conditions, suggesting a restricted, low energy, dysoxic–anoxic depositional environment (Mendonça Filho & Gonçalves, 2017; Mendonça Filho *et al.* 2010; 2012; 2017; Tyson 1995). Dinoflagellate cysts (*Subtilisphaera* spp.) are registered in sample 219.70 m, indicating incipient marine influence. Bobco *et al.* (2023) describes a sedimentary sequence characterized by laminated clay and *Mermia* ichnofabric, interpreting an ephemeral lake, with oxygenated marginal environment and with an anoxic central portion. This central portion could be related to the abundant juvenile ostracod assemblages occurring at discrete levels and showing signs of pyritization. Therefore, a brackish lacustrine environment is interpreted for PI-2.

PI-3 (203 to 182 m) is represented by MA-3, which includes samples 187.70 m, 199.10 m, and 199.40 m. Agglutinated foraminifera are registered in sample 182.50 m, which also contains marine palynomorphs (*Subtilisphaera* spp.), characterizing marine influence at this interval. PF-3 is dominated by Bacterial AOM, and presents the highest TOC (reaching 19.60 wt.% in sample 182.50 m) and TS (reaching 25.01 wt.% in sample 182.05 m) levels in the entire section, suggesting a restricted, saline/hypersaline, low-energy, anoxic depositional environment, with stratified water column, low continental input and low runoff (Mendonça Filho & Gonçalves, 2017; Mendonça Filho *et al.* 2010; 2012; 2017; Tyson 1995). At this interval, the lake reaches its most restrictive conditions and bacterial activity occurs. Primary paleoproductivity in this shallow water body was probably concentrated in the upper photic zone of the water column, where autotrophic photosynthetic bacteria proliferated, producing bacterial mucilage commonly associated with carbonate sedimentation and low IR values (Fonseca *et al.* 2020; Marques-Lima *et al.* 2023;). Bobco *et al.* (2023) registered domal stromatolites and microbial mats at this interval, inferring perennial, restrictive and alkaline conditions and interpreting three depositional stages for it (perennial shallow lake, evaporitic sabkha and stratified lake stages). A restricted hypersaline lake transitioning to an evaporitic-sabkha paleoenvironment can be interpreted for this interval. Marine fossil registered in sample 182.50 m, could possibly indicate a marine ingression related to the end of the evaporitic phase, as interpreted by Salgado-Campos *et al.* (2022).

PI-4 (182 to 166 m) presented no recovery of ostracods or associated fossil material. Nevertheless, PF-1 is represented in sample 170.00 m, which registers a phytoclast and sporomorph dominated level, indicating freshwater environment and oxic regime. This interval is positioned above a probable unconformity which separates the lower Codó from the upper Codó Formation (Bobco *et al.*

CC BY

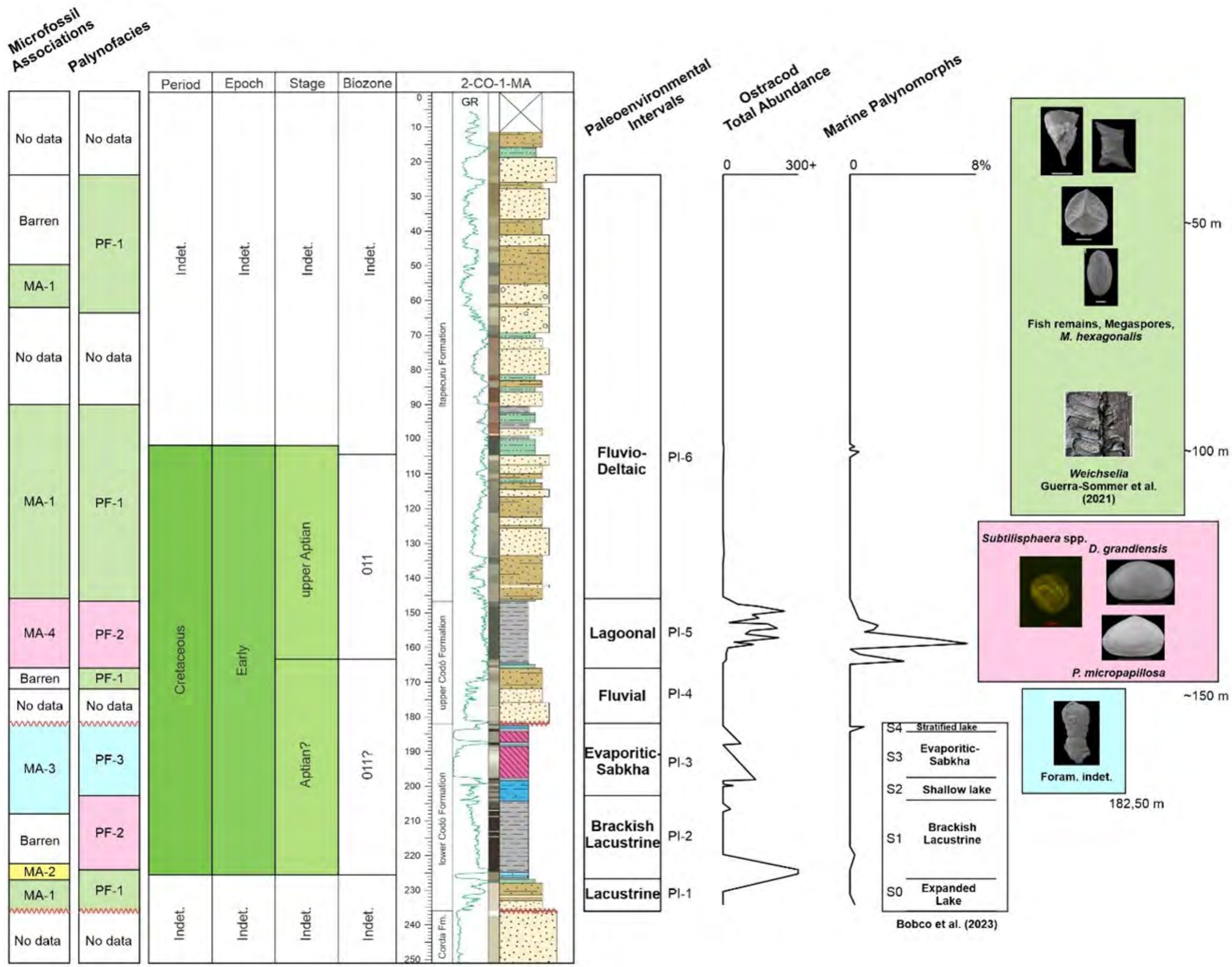

Figure 10 Integration of microfossil associations, palynofacies and interpreted paleoenvironmental intervals. Gamma-ray log (GR) is colored in green.

CC BY

2023; Mendes, 2007). Sandstone intervals lying above probably correlated surfaces which were characterized as unconformities within this lithostratigraphic unit were interpreted as fluvial in the 1-UN-24-PI and 1-UN-32-PI boreholes (Mendes, 2007, Salgado-Campos *et al.* 2022). This interpretation is consistent with PF-1. Therefore, a fluvial paleoenvironment is proposed for this interval.

PI-5 (166 to 146 m) is characterized by MA-4, composed by moderately abundant ostracod assemblages, mainly represented by articulated carapaces of *Damonella grandiensis* late juvenile instars, characterizing a low diversity, high dominance ostracod fauna. That is corroborated by the Shannon Diversity Index values, which are low and irregular, averaging at 0.32, characterizing unfavorable conditions for ostracod species development. Such low diversity characterizes stressed environments, possibly brackish to hypersaline waters, favoring the development of opportunistic species (Antonietto *et al.* 2012; Boomer *et al.* 2003). Additionally, the predominance of articulated juvenile carapaces could be indicative of juvenile mortality due to high salinity, anoxia and other unfavorable conditions (Boomer *et al.* 2003; Whatley 1988).The ostracod fauna is dominated by *Damonella grandiensis*, associated with *Pattersoncypris micropapillosa* and minor occurrences of *Pattersoncypris symmetrica* and *Pattersoncypris* sp. Do Carmo *et al.* (2018) consider those species to be freshwater euryhaline, noting that some of them can tolerate a wide range of salinities, from oligohaline to brackish waters. *Damonella grandiensis* was registered occurring with marine ostracods, foraminifera and nannofossils (Araripe *et al.* 2022; Guzmán *et al.* 2023). The occurrence of *P. micropapillosa* alongside moderate amounts of dinoflagellate cysts in the Santana Formation was interpreted as indicative of the establishment of a mixohaline coastal environment, such as estuaries and lagoons, subjected to pulsative marine influence (Arai & Coimbra 1990). PF-2 is dominated by Terrestrially-Derived AOM and sporomorphs, while dinoflagellate cysts (*Subtilisphaera* spp.) were registered in eight samples from this interval (163.50 to 151.40 m, except sample 160.00 m), reaching 7.76 wt.% in sample 158.40 m. Palynofacies data indicates a restricted, low energy, dysoxic–anoxic depositional environment, brackish-saline, with a proximal source area, input of higher terrestrial plants and incipient marine influence (Mendonça Filho & Gonçalves, 2017; Mendonça Filho *et al.* 2010; 2012; 2017; Tyson 1995). This data allows interpretation of a lagoonal paleoenvironment for the interval.

PI-6 (146 to 24 m) registers MA-1, a microfossil association composed by very rare, fragmented and disarticulated indeterminate ostracods, exhibiting evidence of oxidation and dissolution. Megaspores and *M. hexagonalis* are registered along with fish fragments and freshwater Gastropoda, suggesting a high energy, oxic, proximal freshwater environment subjected to terrigenous input. PF-1 is dominated by phytoclasts and sporomorphs, suggesting a continental freshwater environment, oxic regime, high energy, strongly influenced by higher terrestrial plants (Mendonça Filho & Gonçalves, 2017; Mendonça Filho *et al.* 2010; 2012; 2017; Tyson 1995). Punctual marine influence is registered by the presence of dinoflagellate cysts (*Subtilisphaera* spp.) in samples 102.75 m; 101.75 m; 101.35 m; 101.20 m. Additionally, the remains of fern *Weichselia* and terrestrial bryophytes *Muscites* sp. were identified in this interval, pointing to marginal areas of freshwater bodies subjected to frequent flooding, in a general fluvio-deltaic scenario (Guerra-Sommer *et al.* 2021). This is consistent with previous studies that suggested wet forest paleovegetation and deposition in floodplains in a humid paleoclimate (Ferreira *et al.* 2016; 2020; Menezes *et al.* 2023). As such, a fluvio-deltaic paleoenvironment is proposed for that interval.

5.3 Marine Ingressions

The existence of a pre-evaporitic lower Codó Formation deposited under hypersaline lacustrine conditions and an upper Codó Formation, deposited under variable degree of marine influence was recognized by multiple studies, despite some divergences (Bastos *et al.* 2022; Mendes, 2007; Salgado-Campos *et al.* 2022). Our data reinforces this interpretation, providing additional evidence for it.

Distinct microfaunas are observed below and above the gypsum layer, pointing to different paleoenvironments. A hypersaline alkaline lacustrine system, subject to intense evaporation and arid climate is proposed for the lower Codó Formation in some studies (Bobco *et al.* 2023; Salgado-Campos *et al.* 2022). In that interval, ostracods are represented in markedly lower abundance and worse preservation when compared to the upper part of Codó Formation, a distribution pattern that is also observed in some other studies in this unit (Barros *et al.* 2022; Soldani, 2022). This distribution pattern could be related to the intense evaporation and arid climate, generating extreme hypersaline conditions that could be unfavorable for the development of most ostracod species. Additionally, diagenetic factors could also be at play, hampering preservation of ostracod shells in the lower part of Codó Formation, and explaining the generally bad preservation state registered for the ostracod faunas.Overall, the occurrence of monospecific and paucispecific ostracod faunas composed of species of *Damonella* and *Pattersoncypris* could be explained by cyclic processes of contraction and expansion of the hypersaline lake system which is supposed to have acted during the deposition of the lower portion of the unit, causing proliferation followed by mortality of resistant species (Maizatto *et al.* 2011; Ramos *et al.* 2006). In the upper Codó Formation, the more persistent and abundant occurrence of those resistant ostracod species alongside dinoflagellate cysts (this work) and foraminifera (Barros *et al.* 2022), allows the proposition of a brackish-saline lagoonal paleoenvironment, which could have been less hostile to ostracods, but still did not allow the development of diverse faunas.

The interpretation of data gathered here reinforces the assumption of a connection with the sea during the Codó Formation deposition, particularly for the upper Codó sediments. However, correlation of different sections within the Parnaíba Basin seems to indicate that marine influence varies significantly, being weaker in some localities (Figure 11). In the 2-CO-1-MA borehole, marine influence is punctually observed at discrete levels in the pre-evaporitic succession, incipiently marked by the presence of dinoflagellate cysts, which are more abundant above the gypsum layer, in PI-5, reaching 7.76 %. Marques-Lima *et al.* (2023), who analysed the 2-TV-1-MA borehole, registered punctual occurrences of dinoflagellate cysts in the initial stages of deposition for the Codó Formation, and more significant occurrences above the gypsum layer, reaching 0.3 %. Contrasting with that, other studies report more abundant occurrences, registering the *Subtilisphaera* spp. Ecozone above the gypsum layer and evidencing stronger marine connection (Antonioli & Arai, 2002; Neves, 2007). Adding to that, in the 2-CO-1-MA section, agglutinated foraminifera were registered in a single sample, with low abundance, contrasting with other recent studies that reported more abundant occurrences of foraminifera (1-UN-24-PI; Barros *et al.* 2022), and marine gastropoda (1-UN-32-PI; Soldani, 2022), possibly suggesting stronger marine influence in their respective localities.

Characterizing marine ingressions in the Codó sediments is crucial not only for the paleoenvironmental interpretation, but also when considering hypotheses regarding the establishment of a mid-Cretaceous seaway in Northeastern Brazil (Arai, 2014; Azevedo *et al.* 2024; Bastos *et al.* 2022 and references therein). The correlation presented here (Figure 11) may indicate a distant position relative to the marine source for the 2-CO-1-MA and 2-TV-1-MA boreholes and a complex configuration for the hypothetical narrow seaway. Integrated micropaleontological investigations of other sections within the basin, coupled with basin reconstruction and other techniques, could lead to more precise paleogeographic reconstructions and marine ingression route models, enhancing our understanding of this unique geological setting.

6 Conclusions

We described a fauna and flora with low diversity and moderate to poor preservation, which included megaspores, foraminifera, termite coprolites, gastropoda, fish remains and index species of the *Cytheridea*? spp. 201–218 ostracod Biozone. Coupled with previous findings, this enabled stratigraphic positioning of the studied section in the upper Aptian. The sedimentary succession of the Codó and Itapecuru formations records the evolution of paleoenvironments transitioning from lacustrine, brackish lacustrine, evaporitic-sabkha, fluvial, lagoonal, to fluvio-deltaic settings. Paleontological evidence, including agglutinated foraminifera and dinoflagellate cysts (*Subtilisphaera* spp.), indicates marine ingressions, especially in the upper Codó Formation, with marine influence varying geographically within the Parnaíba Basin.

7 Acknowledgements

We gratefully acknowledge the R&D project registered as “Projeto Alagoas: Correlação estratigráfica, evolução paleoambiental e paleogeográfica e perspectivas exploratórias do Andar Alagoas”, sponsored by Shell Brasil Petróleo Ltda. as part of the “Compromisso com Investimentos em Pesquisa e Desenvolvimento” of Agência Nacional do Petróleo, Gás Natural e Biocombustíveis (ANP), technical cooperation agreement #20219. We are grateful to Centro de Tecnologia Mineral (CETEM/MCTI) for the assistance during the scanning electron microscope imaging procedures. We are also grateful to the Laboratório de Geologia Sedimentar (Lagesed/UFRJ), namely geologists Bruno César Araújo, Fábia Emanuela Bobco, and Professor Leonardo Borghi for providing lithology descriptions for the studied interval (Figure 2) and assistance during sampling procedures. Additionally, we are grateful to Laboratório de Micropaleontologia Aplicada (MicrA/UFRJ), namely geologist Kelly Bonito, for the assistance during sample preparation. Finally, we thank Associate Editor Dr. Hermínio Ismael de Araújo Júnior, reviewer Helena Antunes Portela and one anonymous reviewer for the suggestions and criticisms, which greatly helped to improve this manuscript.

8 Supplementary Material

The following material is available for this article:

Supplementary Material S1. Ostracods.
Supplementary Material S2. Palynofacies.

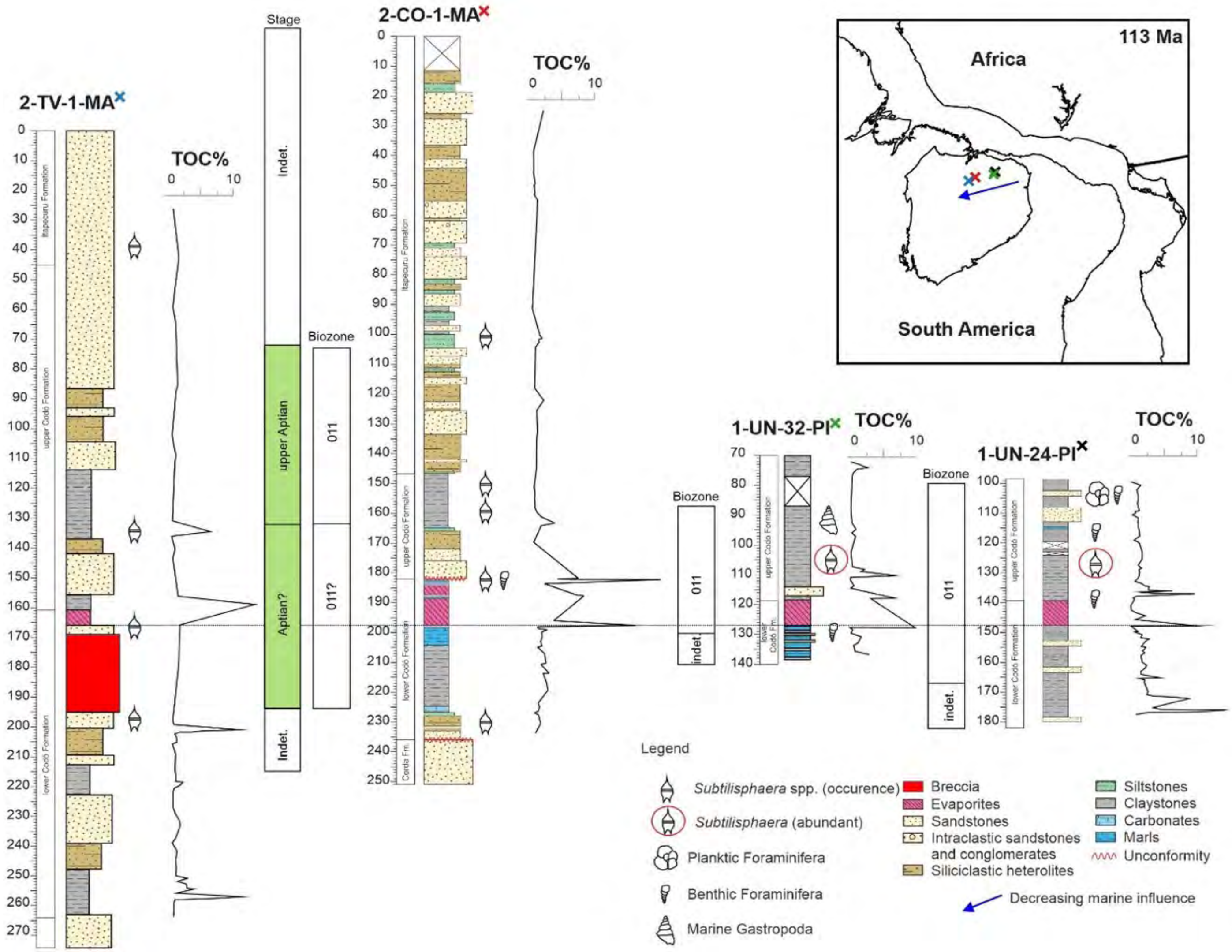

Figure 11 Correlation of four different sections within the Parnaíba Basin: 2-TV-1-MA (adapted from Marque-Lima *et al.* (2023)), 2-CO-1-MA (this work), 1-UN-32-PI (ostracod biozones and paleontology based on Soldani (2022), TOC and dinoflagellate cysts *Subtilisphaera* spp. based on Neves (2007)), 1-UN-24-PI (ostracod biozones and paleontology based on Barros *et al.* (2022), TOC based on Bastos *et al.* (2020) and dinoflagellate cysts *Subtilisphaera* spp. based on Neves (2007)). Paleogeographic schematic map generated with Gplates software (Müller *et al.* 2018).

9 References

Anaisse Júnior, J., Truckenbrodt, W. & Rossetti, D.F. 2001, 'Fácies de um sistema estuarino lagunar no Grupo Itapecuru, área de Açailândia/MA, Bacia do Grajaú', in D.F. Rossetti, A.M. Góes & W. Truckenbrodt (eds.), *O Cretáceo na Bacia de São Luís-Grajaú*, Museu Paraense Emílio Goeldi, Belém, PA, pp. 119–50.

Anderson, F.W. 1966, 'Some British Jurassic and Cretaceous Ostracoda: 1. New genera of Purbeck and Wealden Ostracoda', *Bulletin of the British Museum (Natural History)*, vol. 11, pp. 433–87.

Antonietto, L.S. 2010, 'Ostracodes da Formação Santana (Cretáceo Inferior, Aptiano Superior), Bacia do Araripe, NE-Brasil: taxonomia, distribuição estratigráfica e paleoecologia', Master Thesis, Universidade de Brasília.

Antonietto, L.S., Gobbo, S.R., do Carmo, D.A., Assine, M.L., Fernandes, M.A.M.C.C., Lima e Silva, J.S.E. 2012, 'Taxonomy, ontogeny and paleoecology of two species of Harbinia Tsao, 1959 (Crustacea, Ostracoda) from the Santana Formation, Lower Cretaceous, Northeastern Brazil', *Journal of Paleontology*, vol. 86, no. 4, pp. 659–68, DOI:10.1666/11-012R.1

Antonioli, L. & Arai, M. 2002, 'O registro da Ecozona Subtilisphaera na Formação Codó (Cretáceo Inferior da Bacia do Parnaíba, Nordeste do Brasil): seu significado paleogeográfico', *Proceedings of 6º Simpósio Sobre o Cretáceo do Brasil*, pp. 25–30.

Antunes, R.L., Azevedo, R.L.M. & Lobo, J.T. 2018, 'Reflexões sobre a Série Recôncavo, Brasil', *Anuário do Instituto de Geociências da UFRJ*, vol. 41, pp. 276–96, DOI:10.11137/2018_2_276_296

Arai, M. 2001, 'Palinologia de depósitos cretáceos no Norte e Meio-Norte do Brasil:
histórico e estado-de-arte', in D.F. Rossetti, A.M. Góes, W. Truckenbrodt (eds.), *O Cretáceo na Bacia de São Luís-Grajaú*, Museu Paraense Emílio Goeldi (Coleção Friedrich Katzer), Belém, pp. 31–46.

Arai, M. 2014, 'Aptian/Albian (Early Cretaceous) paleogeography of the South Atlantic: a paleontological perspective', *Brazilian Journal of Geology*, vol. 44, no. 2, pp. 339–50, DOI:10.5327/Z2317-4889201400020012

Arai, M. & Assine, M.L. 2020, 'Chronostratigraphic constraints and paleoenvironmental interpretation of the Romualdo Formation (Santana Group, Araripe Basin, Northeastern Brazil) based on palynology', *Cretaceous Research*, vol. 116, no. 104610, DOI:10.1016/j.cretres.2020.104610

Arai, M. & Coimbra, J.C. 1990, 'Análise Paleoecológica do Registro das Primeiras Ingressões Marinhas na Formação Santana (Cretáceo Inferior da Chapada do Araripe)', in D.A. Campos, M.S.S. Viana, P.M. Brito & G. Beurlen (eds.), *Proceedings of I Simpósio Sobre a Bacia Do Araripe e Bacias Interiores Do Nordeste*, pp. 225–39.

Arai, M., Hashimoto, A.T. & Uesugui, N. 1989, 'Significado Cronoestratigráfico da Associação Microflorística do Cretáceo Inferior do Brasil', *Boletim de Geociências da Petrobras*, vol. 3, pp. 87–103.

Araripe, R.C., Oliveira, D.H., Tomé, M.E., Moura de Mello, R. & Barreto, A.M.F. 2021, 'Foraminifera and Ostracoda from the Lower Cretaceous (Aptian–lower Albian) Romualdo Formation, Araripe basin, northeast Brazil: Paleoenvironmental inferences', *Cretaceous Research*, vol. 122, no. 104766, DOI:10.1016/j.cretres.2021.104766

Araripe, R.C., Pedrosa Lemos, F.A., do Prado, L.A.C., Tomé, M.E.T.R., Oliveira, D.H.D., Pereira, P.A., Nascimento, L.R.S.L., Asakura, Y., Ng, C., Viviers, M.C. & Barreto, A.F. 2022, 'Upper Aptian–lower Albian of the southern-central Araripe Basin, Brazil: Microbiostratigraphic and paleoecological inferences', *Journal of South American Earth Sciences*, vol. 116, no. 103814, DOI:10.1016/j.jsames.2022.103814

ASTM Standard D4239-08. 2008, *Standard Test Methods for Sulfur in the Analysis Sample of Coal and Coke Using High-Temperature Tube Furnace Combustion Methods*, ASTM International, West Conshohocken, PA.

Azevedo, R. L., Antunes, R. L., Bruno, M. D., Fairchild, T. R. & Dias-Brito, D. 2024, 'The Central South Atlantic: The origin of its waters, its evolution and effects beyond', *Carnets Geol.*, vol. 24, pp. 29–74, DOI:10.2110/carnets.2024.2402

Bahniuk, A.M., Anjos, S., França, A.B., Matsuda, N., Eiler, J., Mckenzie, J.A., & Vasconcelos, C. 2015, 'Development of microbial carbonates in the Lower Cretaceous Codó Formation (north-east Brazil): implications for interpretation of microbialite facies associations and palaeoenvironmental conditions', *Sedimentology*, vol. 62, no. 1, pp. 155–81, DOI:10.1111/sed.12144

Baird, W. 1845, 'Arrangement of the British Entomostraca, with a list of species, particularly noticing those which have as yet been discovered within the bounds of the club', *History of the Berwickshire Naturalists' Club*, vol. 2, pp. 145–8.

Barros, C., Silva, S.C., Machado, L.L., Rios-Netto, A. de M., Sames, B., Alves, T.D. & Silva Jr., R.P. 2022, 'Non-marine ostracods of the Codó Formation (upper Aptian, Lower Cretaceous), Parnaíba Basin, NE Brazil: new biostratigraphic and paleoecological insights', *Cretaceous Research*, vol. 133, no. 105125, DOI:10.1016/j.cretres.2021.105125

Bastos, L.P.H., Jagniecki, E.A., Holanda dos Santos, W., da Costa Cavalcante, D., Jorge de Menezes, C., Ferreira Alferes, C.L., Neves da Silva, D.B., Bergamaschi, S., Rodrigues, R. & Pereira, E. 2022, 'Organic geochemical evidence for the transition of Aptian-Albian hypersaline environments into marine restricted seas: The South Atlantic oceanic northern gateway and its implications for the pre-salt deposits', *Marine and Petroleum Geology*, vol. 140, no. 105632, DOI:10.1016/j.marpetgeo.2022.105632

Bastos, L.P.H., Pereira, E., da Costa Cavalcante, D., Alferes, C.L.F., de Menezes, C.J. & Rodrigues, R. 2020, 'Expression of early cretaceous global anoxic events in Northeastern Brazilian basins', *Cretaceous Research*, vol. 110, no. 104390, DOI:10.1016/j. cretres.2020.104390

Bastos, L.P.H., Pereira, E., Cavalcante, D.D.C. & Rodrigues, R. 2014, 'Estratigrafia química aplicada à Formação Codó nos furos de sondagem UN-24-PI e UN-37-PI (Aptiano/Albiano da Bacia do Parnaíba)', *Boletim de Geociências da Petrobras*, vol. 22, pp. 289–312.

Bate, R.H. 1972, 'Phosphatized ostracods with appendages from the Lower Cretaceous of Brazil', *Palaeontology*, vol. 15, pp. 379–93.

Bate, R.H. 1999, 'Non-marine ostracod assemblages of the Pre-Salt rift basins of West Africa and their role in sequence stratigraphy', *Geological Society of London Special Publications*, vol. 153, pp. 283–92, DOI:10.1144/GSL.SP.1999.153.01.17

Bate, R.H., Horne, D.J., Horne, S.E., Douglas, L., Miller, C.G. & Lord, A.R. 2022, 'Non-marine Ostracoda (Crustacea) of the Early Cretaceous 'Pre-Salt' sediments of Brazil: An illustrated catalogue of the type specimens of Wicher, Krömmelbein, Krömmelbein & Weber, and Bate', *Zootaxa*, vol. 5098, pp. 1–84, DOI:10.11646/zootaxa.5098.1.1

Batista, A.M.N. 1992, 'Caracterização paleoambiental dos sedimentos Codó-Grajaú, Bacia de São Luís (MA)', Master Thesis, Universidade Federal do Pará.

Batten, D.J. & Stead, D.T. 2005, 'Palynofacies Analysis and its Stratigraphic Application', in E.A.M. Koutsoukos (ed.), *Applied Stratigraphy, Topics in Geobiology*, Springer Netherlands, pp. 203–26, DOI:10.1007/1-4020-2763-X_10

Bobco, F.E.R., Trombetta, M.C., Ferreira, L.O., Silveira, L.F., Kroth, M., Mendonça, J.O., Mendonça Filho, J.G., Sedorko, G., Araujo, B.C. & Borghi, L. 2023, 'Alternations of open and closed lakes in the Lower Aptian Codó Formation (Parnaíba Basin, Brazil)', *Sedimentary Geology*, vol. 455 (2023), no. 106478, DOI:10.1016/j.sedgeo.2023.106478

Bom, M.H.H., Ceolin, D., Kochhann, K.G.D., Krahl, G., Fauth, G., Bergue, C.T., Savian, J.F., Strohschoen Junior, O., Simões, M.G. & Assine, M.L. 2021, 'Paleoenvironmental evolution of the Aptian Romualdo Formation, Araripe Basin, Northeastern Brazil. Global and Planetary Change', vol. 203, no. 103528, DOI:10.1016/j.gloplacha.2021.103528

Boomer, I. & Eisenhauer, G. 2002, 'Ostracod faunas as palaeoenvironmental indicators in marginal marine environments', in J.A. Holmes, A.R. Chivas (eds.), *The Ostracoda: Applications in Quaternary Research*, pp. 135–49, DOI:10.1029/131GM07

Boomer, I., Horne, D.J. & Slipper, I.J. 2003, 'The Use of Ostracods in Palaeoenvironmental Studies, or What can you do with an Ostracod Shell?', *The Paleontological Society Papers*, vol. 9, pp. 153–80, DOI:10.1017/S1089332600002199

Caputo, M.V. 1984, 'Stratigraphy, Tectonics, Paleoclimatology and Paleogeography of Northern Basins of Brazil', PhD Thesis, University of California.

Carbonel, P., Colin, J.P., Danielopol, D.L., Löffler, H. & Neustrueva, I. 1988, 'Paleoecology of limnic ostracodes: A review of some major topics', *Palaeogeography, Palaeoclimatology, Palaeoecology*, vol. 62, pp. 413–61, DOI:10.1016/0031-0182(88)90066-1

Coimbra, J.C., Arai, M. & Carreño, A.L. 2002, 'Biostratigraphy of Lower Cretaceous Microfossils from the Araripe Basin, Northeastern Brazil', *Geobios*, vol. 35, pp. 687–98, DOI:10.1016/S0016-6995(02)00082-7

Coimbra, J.C. & Freire, T.M. 2021, 'Age of the Post-rift Sequence I from the Araripe Basin, Lower Cretaceous, NE Brazil: implications for spatio-temporal correlation', *Revista Brasileira de Paleontologia*, vol. 24, pp. 37–46, DOI:10.4072/rbp.2021.1.03

Colin, J. P., Néraudeau, D., Nel, A. & Perrichot, V. 2011, 'Termite coprolites (Insecta: Isoptera) from the Cretaceous of western France: A palaecological insight', *Revue de micropaléontologie*, vol. 54, pp. 129–139, DOI:10.1016/j.revmic.2011.06.001

Corrêa-Martins, F.J., Mendes, J.C., Bertolino, L.C. & Mendonça, J.O. 2019, 'Petrografia, diagênese e considerações sobre proveniência da Formação Itapecuru no Norte do Maranhão (Cretáceo Inferior, Bacia do Parnaíba, NE Brasil)', *Anuário do Instituto de Geociências da UFRJ*, vol. 41, pp. 514–30, DOI:10.11137/2018_3_514_530

Cunha, F.M.B. 1986, 'Evolução paleozóica da Bacia do Parnaíba e seu arcabouço tectônico', Master Thesis, Universidade Federal do Rio de Janeiro.

D'Souza, L.S. 2020, 'Evolução Tectônica e Estratigráfica Pós Paleozoica da Porção Nordeste da Bacia do Parnaíba e da Bacia de São Luís, Brasil', Master Thesis, Universidade Federal do Rio de Janeiro.

Dennison, J.M. & Hay, W.W. 1967, 'Estimating the needed sampling area for subaquatic ecologic studies', *Journal of Paleontology*, vol. 41, pp. 706–8.

Do Carmo, D.A., Coimbra, J.C., Whatley, R.C., Antonietto, L.S. & De Paiva Citon, R.T. 2013, 'Taxonomy of limnic Ostracoda (Crustacea) from the Alagamar Formation, middle-upper Aptian, Potiguar Basin, northeastern Brazil', *Journal of Paleontology*, vol. 87, pp. 91–104, DOI:10.1666/11-108R.1

Do Carmo, D.A., Spigolon, A.L.D., Guimarães, E.M., Richter, M., Mendonça-Filho, J.G., Dangpeng, X., Caixeta, G.M. & Leite, A.M. 2018, 'Palaeoenvironmental assessment of Early Cretaceous limnic ostracods from the Alagamar Formation, Potiguar Basin, NE Brazil', *Cretaceous Research*, vol. 85, pp. 266–279 DOI:10.1016/j.cretres.2018.01.009

Do Carmo, D.A., Whatley, R., Queiroz Neto, J.V. & Coimbra, J.C. 2008, 'On the Validity of Two Lower Cretaceous Non-marine Ostracode Genera: Biostratigraphic and Paleogeographic Implications', *Journal of Paleontology*, vol. 82, pp. 790–9, DOI:10.1666/07-008.1

Fatela, F. & Taborda, R. 2002, 'Confidence limits of species proportions in microfossil assemblages', *Marine Micropaleontology*, vol. 45, pp. 169–74, DOI:10.1016/S0377-8398(02)00021-X

Fernandes, G. & Della Piazza, H. 1978, 'O Potencial Oleogenítico da Formação Codó', *Boletim Técnico da Petrobras*, vol. 21, pp. 3–16.

Ferreira, N.N., Ferreira, E.P., Ramos, R.R.C. & Carvalho, I.S. 2016, 'Palynological and sedimentary analysis of the Igarapé Ipiranga and Querru 1 outcrops of the Itapecuru Formation (Lower Cretaceous, Parnaíba Basin), Brazil', *Journal of South American Earth Sciences*, vol. 66, pp. 15–31, DOI:10.1016/j.jsames.2015.12.005

Ferreira, N.N., Ferreira, E.P., Ramos, R.R.C. & Carvalho, I. S. 2020, 'Terrestrial and marine palynomorphs from deposits of the pull-apart rift of West Gondwana (Parnaíba Basin, northern Brazil): Biostratigraphy and relation to tectonic events', *Journal of South American Earth Sciences*, vol. 101, no. 102612, DOI:10.1016/j.jsames.2020.102612

Fonseca, C., Mendonça Filho, J.G., Lézin, C. & Duarte, L.V. 2020, 'Organic facies variability and paleoenvironmental changes on the Moroccan Atlantic coast across the Cenomanian-Turonian Oceanic Anoxic Event (OAE2)', *International Journal of Coal Geology* 230, 103587, DOI:10.1016/j.coal.2020.103587

Góes, A.M. 1995, 'A Formação Poti (Carbonífero inferior) da Bacia do Parnaíba', PhD Thesis, Universidade de São Paulo.

Góes, A.M. & Coimbra, A.M. 1996, 'Bacias sedimentares da província sedimentar do meio-norte do Brasil', *Boletim de Resumos Expandidos do Simpósio de Geologia da Amazônia*, vol. 5, pp.186–7.

Góes, A.M. & Feijó, F.J. 1994, 'Bacia do Parnaíba', *Boletim de Geociências da Petrobras*, vol. 8, pp. 57–68.

Góes, A.M., Rossetti, D.F. 2001, 'Gênese da Bacia de São Luís-Grajaú, Meio-Norte do Brasil', in D.F. Rossetti, A.M. Góes & W. Truckenbrodt (eds.), *O Cretáceo Na Bacia de São Luís-Grajaú*, Museu Paranaense Emílio Goeldi, Belém-PA, pp. 15–29.

Grosdidier, E., Braccini, E., Dupont, G., Moron, J.-M. 1996, 'Biozonation du Crétacé Inférieur non marin des bassins du Gabon et du Congo', in S. Jardine, I. De Klasz & J.P. Debeney (eds.), *Géologie de l'Afrique et de l'Atlantique Sud: Bulletin Recherches Exploration-Production Elf-Aquitaine, Mémoire*, Elf Aquitaine, Angers, pp. 67–82.

Guerra-Sommer, M., Degani-Schmidt, I., Mendonça, J.O., Mendonça Filho, J.G., Lopes, F.D.S., Salgado-Campos, V.M.J., Araújo, B. & Carvalho, I.S. 2021, 'Multidisciplinary approach as a key for paleoenvironmental interpretation in a Weichselia-dominant interval from the late Aptian Codó Formation (Parnaíba Basin, Brazil)', *Journal of South American Earth Sciences*, vol. 111, no. 103490,DOI:10.1016/j.jsames.2021.103490

Guzmán, J., Piovesan, E. K., Almeida-Lima, D.S., Sousa, A. J. & Neumann, V.H.M.L. 2022, 'Aptian ostracods from the Santana Group, Araripe Basin, Brazil', *Revue de micropaléontologie*, vol. 77 (2022), no. 100692, DOI:10.1016/j.revmic.2022.100694

Guzmán, J., Piovesan, E.K., Melo, R.M., Almeida-Lima, D., Sousa, A. J. & Neumann, V.H.M.L. 2023, 'Ostracoda and foraminífera biostratigraphy and palaeoenvironmental evolution of the Aptian Santana Group, post-rift of the Araripe Basin, Brazil', *Gondwana Research*, vol. 124 (2023), pp. 18–23,DOI:b10.1016/j.gr.2023.06.014

Hammer, O., Harper, D.A. & Ryan, P.D. 2001, 'PAST: paleontological statistics software package for education and data analysis', *Palaeontologia Electronica*, vol. 4, no. 1, pp. 1–9.

Horne, D.J. 2005, 'Ostracoda', in R.C., Selley, L.R.M. Cocks & I.R. Plimer (eds.), *Encyclopedia of Geology*, Elsevier, Oxford, pp. 453–63, DOI:10.1016/B0-12-369396-9/00511-6

Kaufmann, A. 1900, 'Cypriden und Darwinuliden der Schweiz', *Revue Suisse de Zoologie*, vol. 8, pp. 209–423, DOI:10.5962/bhl.part.10584

Krömmelbein, K. & Weber, R. 1971, 'Ostracoden des Nordost-Brasilianischen Wealden', *Beihefte zum' Geologischen Jahrbuch*, vol. 115, pp. 1–93.

Latreille, P.A. 1802, 'Histoire naturelle, générale et particulière des Crustacés et des Insectes', *Histoires des Cypris et des Cytherées*, vol. 8, pp. 232–54.

Lima, H.P., Aranha, L.G.F. & Feijó, F.J. 1994, 'Bacias de Bragança-Viseu, São Luíz e Graben de Ilha Nova', *Boletim de Geociências da Petrobras*, vol. 8, pp. 111–116.

Lima, M.R. 1982, 'Palinologia da Formação Codó na região de Codó, Maranhão', *Boletim do Instituto de Geociências da USP*, vol. 13, pp. 116–128, DOI:10.11606/issn.2316-8978.v13i0p116-128

Lindoso, R.M., Carvalho, I.S. & Mendes, I.D. 2013, 'An isopod from the Codó Formation (Aptian of the Parnaíba Basin), Northeastern Brazil', *Brazilian Journal of Geology*, vol 43, no. 1, pp. 16–21, DOI:b10.5327/Z2317-48892013000100003

Lindoso, R.M., Maisey, J.G. & Carvalho, I.S. 2016, 'Ichthyofauna from the Codó Formation, Lower Cretaceous (Aptian, Parnaíba Basin), Northeastern Brazil and their paleobiogeographical and paleoecological significance', *Palaeogeography, Palaeoclimatology, Palaeoecology*, vol. 447 (2016), pp. 53–64, DOI:10.1016/j.palaeo.2016.01.045

Lúcio, T., Souza Neto, J.A. & Selby, D. 2020, 'Late Barremian/Early Aptian Re-Os age of the Ipubi Formation black shales: Stratigraphic and paleoenvironmental implications for Araripe Basin, northeastern Brazil', *Journal of South American Earth Sciences*, vol. 102, 102699, DOI:10.1016/j.jsames.2020.102699

Maizatto, J.R., Queiroz Neto, J.V., Ferreira, E.P. & Bahniuk, A.M. 2011, 'Palinomorfos e ostracodes não marinhos de afloramentos da Formação Codó, Bacia do Parnaíba', in I.S. Carvalho, N.K. Srivastava, O.S. Strohschoen Jr. & C.C. Lana (eds.), *Paleontologia: Cenários de Vida*, Editora Interciência, pp. 367–378.

Marques-Lima, D., Mendonça-Filho, J.G., Fonseca, C., Oliveira, A. D., Mendonça, J. O. & Gonçalves, P.A. 2023, 'Organic facies variability and paleoenvironmental characterization of the Codó and Itapecuru formations (Aptian–Albian) of Parnaíba Basin, Brazil', *International Journal of Coal Geology*, vol. 277 (2023), no. 104337, DOI:10.1016/j.coal.2023.104337

McLoughlin, S., Santos, A.A., Donaldson, S., Pott, C. & Mccurry, M.R. 2024, 'Termite activity in the mid-Cretaceous of Australia', *Palaeontologia Electronica*, vol. 27.

Melo, R.M., Guzmán, J., Almeida-Lima, D., Piovesan, E.K., Neumann, V.H. de M.L. & Sousa, A. 2020, 'New marine data and age accuracy of the Romualdo Formation, Araripe Basin, Brazil', *Scientific Reports*, vol. 10, no. 15779, DOI:10.1038/s41598-020-72789-8

Mendes, M.S. 2007, 'Análise estratigráfica do intervalo formacional Grajaú–Codó (Aptiano) da bacia do Parnaíba, NE do Brasil', Master Thesis, Universidade Federal do Rio de Janeiro.

Mendonça Filho, J.G. & Gonçalves, P.A. 2017, 'Organic matter: concepts and definitions', in I. Suárez-Ruiz & J.G. Mendonça Filho (eds.), *Geology: Current and Future Developments. The Role of Organic Petrology in the Exploration of Conventional and Unconventional Hydrocarbon Systems, vol. 1.*, Bentham Science Publishers, United Arab Emirates, pp. 1–33.

Mendonça Filho, J.G., Menezes, T.R., Mendonça, J.O., Oliveira, A.D., Carvalho, M.A., Sant'Anna, A.J. & Souza, J.T. 2010, 'Palinofácies', in I.S. Carvalho (ed.), *Paleontologia*, Rio de Janeiro, Interciência, vol. 2, pp. 379–413.

Mendonça Filho, J.G., Menezes, T.R., Mendonça, J.O., Oliveira, A.D., Silva, T.F., Rondon, N.F. & Silva, F.S. 2012, 'Organic Facies: Palynofacies and Organic Geochemistry Approaches', in D. Panagiotaras (ed.), *Geochemistry Earth's System Processes*, Rijeka, InTech, pp. 211–48.

Mendonça Filho, J.G.; Menezes, T.R. & Mendonça, J.O. 2017, '10th ICCP Training Course on Dispersed Organic Matter Integrating Transmitted and Reflected Light Microscopy, GFZ (Deutsches GeoForschungsZentrum)', Potsdam, Germany, ISBN 978-84-697-4419-2.

Menezes, M.N., Araújo-Júnior, H.I. & Dal' Bó, P.F. 2019, 'Integrating ichnology and paleopedology in the analysis of Albian alluvial plains of the Parnaíba Basin, Brazil', Cretaceous Research, vol. 96, pp. 210–226, DOI:10.1016/j.cretres.2018.12.013

Menezes, M.N., Dal' Bó, P.F., Smith, J.J., Borghi, L., Arena, M., Favoreto, J. & Araújo-Júnior, H.I. 2023, 'Pedogenic processes and climatic conditions from Cretaceous (Albian) tropical paleosols of the Itapecuru Formation, Parnaíba Basin, northeast Brazil', Palaeogeography, Palaeoclimatology, Palaeoecology, 633, 111881, DOI:10.1016/j.palaeo.2023.111881

Mesner, J.C. & Wooldridge, L.C. 1964, 'Estratigrafia das bacias paleozóica e cretácea do Maranhão', *Boletim Técnico da Petrobras*, vol. 7, pp. 137–164.

Milani, E.J., Rangel, H.D., Bueno, G.V., Stica, J.M., Winter, W.R., Caixeta, J.M. & Neto, O.P. 2007, 'Bacias sedimentares brasileiras: cartas estratigráficas', *Boletim de Geociências da Petrobras*, vol. 15, pp. 183–205.

Moura, J.A. 1988, 'Ostracods from Non-marine Early Cretaceous Sediments of the Campos Basin, Brazil', *Developments in Palaeontology and Stratigraphy*, pp. 1207–1216, DOI:b10.1016/S0920-5446(08)70250-4

Müller, R. D., Cannon, J., Qin, X., Watson, R. J., Gurnis, M., Williams, S., Pfaffelmoser, T., Seton, M., Russell, S. H. J. & Zahirovic, S. 2018, 'GPlates: Building a virtual Earth through deep time', *Geochemistry, Geophysics, Geosystems*, vol. 19, no. 7, pp. 2243–61, DOI:10.1029/2018GC007584

Nascimento, L.R.D.S.L., Tomé, M.E.T.R., Barreto, A.M.F., Holanda de Oliveira, D. & Neumann, V.H.M.L. 2017, 'Biostratigraphic analysis based on palynomorphs and ostracods from core 2-JNS-01PE, Lower Cretaceous, Jatobá Basin, northeastern Brazil', *Journal of South American Earth Sciences*, vol. 76, pp. 115–36, DOI:10.1016/j.jsames.2017.02.012

Neale, J.W. 1988, 'Ostracoda and Palaeosalinity Reconstruction', in P. Deckker, J.P. Colin, J.P. Peypouquet (eds.), *Ostracoda in the Earth Sciences*, Elsevier Science Publishing Co., Inc., Amsterdam, Holanda, pp. 126–55.

Neumann, V.H.M.L. 1999, 'Estratigrafía, sedimentología, geoquímica y diagénesis de los sistemas lacustres aptiense-albienses de la Cuenca de Araripe (Noreste de Brasil)', PhD Thesis, Universitat de Barcelona.

Neves, I.A.N. 2007, 'Aplicação da palinofacies na caracterização paleoambiental da Formação Codó, Cretáceo da Bacia do Parnaíba', Bachelor Thesis, Universidade Federal do Rio de Janeiro.

Oliveira, A.D., Mendonça Filho, J.G., Carvalho, M.A., Menezes, T.R., Lana, C.C. & Brenner, W.W. 2004, 'Novo método de preparação palinológica para aumentar a recuperação de dinoflagelados', *Revista Brasileira de Paleontologia* vol. 7, pp. 169–75, DOI:10.4072/rbp.2004.2.09

Ősi, A., Szabó, M., Tóth, E., Bodor, E., Lobitzer, H., Kvaček, J., Svobodová, M., Szente, I., Wagreich, M., Trabelsi, K., Sames, B., Magyar, J., Makádi, L., Berning, B. & Botfalvai, G. 2021, 'A brackish to non-marine aquatic and terrestrial fóssil assemblage with vertebrates from the lower Coniacian (Upper Cretaceous) Gosau Group of the Tiefengraben locality near St. Wolfgang im Salzkammergut, Austria', *Cretaceous Research*, vol. 127, no. 104938.

Paz, J.D.S. & Rossetti, D.F. 2001, 'Reconstrução paleoambiental da Formação Codó (Aptiano), borda leste da Bacia do Grajaú, MA', in D.F. Rossetti, A.M. Góes & W. Truckenbrodt (eds.), *O Cretáceo Na Bacia de São Luís-Grajaú*, Museu Paranaense Emílio Goeldi, Belém-PA, pp. 77–100.

Paz, J.D.S., Rossetti, D.F. & Macambira, M.J.B. 2005, 'An Upper Aptian saline pan/lake system from the Brazilian equatorial margin: integration of facies and isotopes', *Sedimentology*, vol. 52, pp. 1303–21, DOI:10.1111/j.1365-3091.2005.00744.x

Pedrão, E. 1995. 'Palinoestratigrafia e evolução paleoambiental de rochas sedimentares aptianas-cenomanianas das bacias de Bragança-Viseu e São Luís', Ph.D. thesis, Universidade Federal do Rio de Janeiro, 225 pp.

Pedrão, E., Barrilari, I.M.R. & Lima, H.P. 1993, *Estudos palinológicos dos sedimentos*

cretáceos da bacia do Parnaíba, CENPES/DIVEX/Petrobrás, Relatório Interno, 40 pp.

Pires, E.F. & Sommer, M.G. 2009, 'Plant–arthropod interaction in the early Cretaceous (Berriasian) of the Araripe Basin, Brazil', *Journal of South American Earth Sciences*, vol. 27, no. 1, pp. 50–59.

Poropat, S.F. & Colin, J.P. 2012a, 'Early Cretaceous ostracod biostratigraphy of eastern Brazil and western Africa: An overview', *Gondwana Research*, vol. 22, pp. 772–98, DOI:10.1016/j.gr.2012.06.002

Poropat, S.F. & Colin, J.P. 2012b, 'Reassessment of the Early Cretaceous non-marine ostracod genera Hourcqia Krömmelbein, 1965 and Pattersoncypris Bate, 1972 with the description of a new genus, Kroemmelbeincypris', *Journal of Paleontology*, vol. 86, pp. 699–719, DOI:10.1666/11-140R.1

Ramos, M.I., Rossetti, D.F. & Paz, J.D.S. 2006, 'Caracterização e significado paleoambiental da fauna de ostracodes da Formação Codó (Neoaptiano), leste da bacia de Grajaú, MA, Brasil', *Revista Brasileira de Paleontologia*, vol. 9, pp. 339–48, DOI:10.4072/rbp.2006.3.09

Regali, M.S.P. & Viana, C.F. 1989, 'Sedimentos do Neojurássico-Eocretáceo do Brasil - Idade e Correlação com a Escala Internacional', Centro de Desenvolvimento de Recursos Humanos Sudeste/Serviço de Desenvolvimento de Recursos Humanos/Petróleo Brasileiro S.A.

Rios-Netto, A. de M., Regali, M. da S.P., Carvalho, I. de S. & Freitas, F.I. 2012, 'Palinoestratigrafia do intervalo Alagoas da Bacia do Araripe, nordeste do Brasil', *Revista Brasileira de Geociências*, vol. 42, pp. 331–42.

Rodrigues, R. 1995, 'A geoquímica orgânica na Bacia do Parnaíba', PhD Thesis, Universidade Federal do Rio Grande do Sul.

cc BY

Rossetti, D.F., Góes, A.M. & Arai, M. 2001, 'A passagem do Aptiano-Albiano na Bacia do Grajaú, MA', in D.F. Rossetti, A.M. Góes & W. Truckenbrodt (eds.), *O Cretáceo Na Bacia de São Luís-Grajaú*, Museu Paranaense Emílio Goeldi, Belém-PA, pp. 100–7.

Rossetti, D.F., Paz, J.D. & Góes, A.M. 2004, 'Facies analysis of the Codó formation (late Aptian) in the Grajaú area, southern São Luís-Grajaú Basin', *Anais da Academia Brasileira de Ciências*, vol. 76, no. 4, pp. 791–806, DOI:10.1590/S000137652004000400012

Salgado-Campos, V.M.J., Carvalho, I.S., Bertolino, L.C., Borghi, L., de Rios-Netto, A.M., Araújo, B.C., Souza, D.C., de Ferreira, L.O. & Bobco, F.E.R. 2022, 'Unraveling an alcaline lake and a climate change in Northeastern Brazil during the Late Aptian', *Sedimentary Geology*, vol. 442, no. 106290, DOI:10.1016/j.sedgeo.2022.106290

Santos, B.C., Lemos, F.P., Araripe, R.V.C., Tomé, M.E., Nascimento, L.R.L., Fernandes, B., Welle, T., Alves, C.F., Barreto, A.F. & Lima Filho, M. 2024, 'Faciological analysis of the Codó Formation (Aptian) in the Grajaú Basin of northeastern Brazil: Records of marine ingressions, and their bioestratigraphic and paleogeographic implications', *Journal of South American Earth Sciences*, vol. 147, pp. 105076, DOI: 10.1016/j.jsames.2024.105076

Sars, G.O. 1866, 'Oversigt af Norges marine ostracoder', *Det Norske Videnskaps-Akademi Forhandlingar*, pp. 1–130.

Schaller, H. 1969, 'Revisão estratigráfica da Bacia de Sergipe/Alagoas', *Boletim Técnico da Petrobras*, vol. 12, pp. 21–86.

Sieger, R. & Grobe, H. 2013, PanPlot 2 - software to visualize profiles and time series. Alfred Wegener Institute, Helmholtz Centre for Polar and Marine Research, Bremerhaven, PANGAEA, DOI: 10.1594/PANGAEA.816201

Silva-Teles Jr., A.C. & Viana, M.S.S. 1990, 'Paleoecologia dos Ostracodes da Formação Santana (Bacia do Araripe): Um Estudo Ontogenético de Populações', *Proceedings of I Simpósio sobre a Bacia do Araripe e Bacias Interiores do Nordeste*, pp. 309–321.

Smith, R.J. 2000, 'Morphology and Ontogeny of Cretaceous Ostracods with Preserved Appendages from Brazil', *Palaeontology*, vol. 43, pp. 63–98, DOI:b10.1111/1475-4983.00119

Sohn, I.G. 1961, 'Techniques for Preparation and Study of Fossil Ostracodes', in R.C. Moore (ed.), *Treatise on Invertebrate Paleontology*, Geological Society of America, pp. 64–70.

Soldani, T.S. 2022, 'Ostracodes da Formação Codó no poço 1-UN-32-PI, Andar Alagoas da Bacia do Parnaíba, NE do Brasil: Taxonomia, Bioestratigrafia e Interpretações Paleoambientais', Bachelor Thesis, Universidade Federal do Rio de Janeiro.

Sousa, E. da S., Júnior, G.R.S., Silva, A.F., Reis, F. de A.M., Sousa, A.A.C. de, Cioccari, G.M., Capilla, R., Souza, I.V.A.F. de, Imamura, P.M., Rodrigues, R., Lopes, J.A.D. & Lima, S.G. 2019, 'Biomarkers in Cretaceous sedimentary rocks from the Codó Formation - Parnaíba Basin: Paleoenvironmental assessment', *Journal of South American Earth Sciences*, vol. 92, pp. 265–81, DOI:10.1016/j.jsames.2019.03.025

Tomé, M.E.T.R., Lima Filho, M.F. & Neumann, V.H.M.L. 2014, 'Taxonomic studies of non-marine ostracods in the Lower Cretaceous (Aptian–lower Albian) of post-rift sequence from Jatobá and Araripe basins (Northeast Brazil): Stratigraphic implications', *Cretaceous Research*, vol. 48, pp. 153–76, DOI:10.1016/j.cretres.2013.12.007

Traverse, A. 2007, *Paleopalynology*, Springer Netherlands, Dordrecht, DOI:10.1007/978-1-4020-5610-9

Tyson, R.V. 1995, *Sedimentary Organic Matter. Organic facies and palynofacies*, Chapman and Hall, London.

Tyson, R.V., Esherwood, P. & Pattison, K.A. 2005, 'Organic facies variations in the Valanginian-mid-Hauterivian interval of the Agrio Formation (Chos Malal area, Neuquén, Argentina): local significance and global context', *Geol. Soc. Lond., Special Publications*, vol. 252, no. 1, pp. 251–66.

Valentin, J.L. 2000, *Ecologia Numérica*, Interciência, Rio de Janeiro.

Vangerow, E.F. 1954, 'Megasporen und andere pflanzliche Mikrofossilien aus der Aachener Kreide', *Palaeontographica Abteilung*, vol. B, pp. 24–38.

Vasconcelos, A.M., Ribeiro, J.A.P., Colares, J.Q.S., Gomes, I.P., Forgiarini, L.L. & Medeiros, M.F. 2004, 'Folha Teresina SB.23', in C. Schobbenhaus, J.H. Gonçalves, J.O.S Santos, M. B. Abram, R. Leão Neto, G.M.M. Matos, R.M. Vidotti, M.A.B. Ramos, J.D.A. de Jesus (eds), *Carta Geológica do Brasil ao Milionésimo*, Sistema de Informações Geográficas, Programa Geologia do Brasil. CPRM, Brasília (CD-ROM).

Vaz, P.T., Rezende, N., Wanderley Filho, J.R. & Travassos, W.S. 2007, 'Bacia do Parnaíba', *Boletim de Geociências da Petrobras*, vol. 15, pp. 253–63.

Whatley, R.C. 1988, 'Population structure of ostracods: some general principles for the recognition of palaeoenvironments', in P. DeDeckker, J.P. Colin & J.P. Peypouquet (eds), *Ostracoda in the Earth Sciences*, Elsevier, Amsterdam, pp. 245–56.

Appendix

Ostracod Taxonomic Notes

Class OSTRACODA Latreille, 1802
Order PODOCOPIDA Sars, 1866
Superfamily CYPRIDOIDEA Baird, 1845
Family CANDONIDAE Kaufmann, 1900
Genus *Damonella* Anderson, 1966

Damonella grandiensis Tomé *et al.*, 2014
(Figure 3, A–C)

1990 Gen. ind. sp. 207: Silva-Telles & Viana, pl. 2, Fig. 2.
1999 Ostracode 207: Neumann, p. 93, Fig. 2 and 4.
2002 Ostracode 207: Coimbra *et al.*, p. 691, Fig. 4, 31.
2006 *Candona* sp.: Ramos *et al.*, p. 344, Fig. 4, Z, Z', Z".
2013 *Candona*? sp.: Do Carmo *et al.*, p. 98, Fig. 5, 12–14.
2014 *Damonella grandiensis*: Tomé *et al.*, p. 165, Fig. 10, A–F.
2017 *Damonella grandiensis*: Nascimento *et al.*, p.124, Fig. 9, K.
2022 *Damonella grandiensis* Barros *et al.*, p.7, Fig. 4, B and C.
2022 *Damonella grandiensis* Guzmán *et al.*, p. 6, Fig. 3, G–I.

Stratigraphic and geographic distribution: Araripe Basin, Santana Formation, Ceará State, Brazil, Aptian (Coimbra *et al.*, 2002; Guzmán *et al.*, 2022; Neumann, 1999; Silva-Telles Jr. & Viana, 1990; Tomé *et al.*, 2014). Potiguar Basin, Alagamar Formation, Rio Grande do Norte State, Brazil, Aptian (Do Carmo *et al.*, 2013). Jatobá Basin, Serra Negra, Pernambuco State, Brazil, Aptian (Nascimento *et al.*, 2017; Tomé *et al.*, 2014). Parnaíba Basin, Codó Formation, Maranhão State, Brazil, Aptian (Barros *et al.*, 2022; Ramos *et al.*, 2006; this work).

Family CYPRIDIDAE Baird, 1845
Subfamily CYPRIDINAE Baird, 1845
Genus *Pattersoncypris* Bate, 1972

Remarks: Krömmelbein & Weber (1971) described four subspecies of *Hourcqia angulata* (*H. a. angulata*; *H. a. sinuata*; *H. a. symmetrica* and *H. a. salitrensis*). Subsequently, Bate (1972) proposed the genus *Pattersoncypris* and described the type species *Pattersoncypris micropapillosa*, also transferring two of the *Hourcqia angulata* subspecies proposed by Krömmelbein & Weber (1971) to that new genus. Do Carmo *et al.* (2008) elevated the four subspecies of *Hourcqia angulata* to species level, and, along with *Pattersoncypris micropapillosa*, assigned them to the genus *Harbinia*. Poropat & Colin (2012b) rejected such assignment, refining the diagnosis of *Pattersoncypris*, while also erecting the new genus *Kroemmelbeincypris*. Guzmán *et al.* (2022) present a revised taxonomic scheme, as well as a complete discussion on the use of genera *Pattersoncypris*, *Hourcqia* and *Harbinia*. The authors of that study also considered the genus *Kroemmelbeincypris* to be invalid. The assignment of *Pattersoncypris micropapillosa*, *Pattersoncypris symmetrica* and *Pattersoncypris* sp. to the *Pattersoncypris* genus is adopted here.

Pattersoncypris micropapillosa Bate, 1972
(Figure 3, D–F)

1972 *Pattersoncypris micropapillosa*: Bate, p. 379–393, pls. 66–71.
1990 *Pattersoncypris micropapillosa*: Arai & Coimbra, p. 239, 2.
2000 *Pattersoncypris micropapillosa*: Smith, pls. 1–9.
2006 *Harbinia micropapillosa*: Ramos *et al.*, p. 344, Fig. 4, A–D.
2008 *Harbinia micropapillosa*: Do Carmo *et al.*, p. 795, Fig. 6, 6.
2010 *Harbinia micropapillosa*: Antonietto, p. 25, Fig. 13, 10.
2012b *Pattersoncypris micropapillosa*: Poropat & Colin, p. 708, Fig. 4, 1.
2014 *Pattersoncypris micropapillosa*: Tomé *et al.*, p. 165, Fig. 10, J–P.
2020 *Pattersoncypris micropapillosa*: Melo *et al.*, p. 9, Fig. 5.
2021 *Harbinia micropapillosa*: Bom *et al.*, p. 5, Fig. 3, C–D.
2022 *Harbinia micropapillosa*: Barros *et al.*, p. 5, Fig. 3, G–H.
2022 *Pattersoncypris micropapillosa*: Bate *et al.*, p. 84, Fig. 14, 1a–1d.
2022 *Pattersoncypris micropapillosa*: Guzmán *et al.*, p. 11, Fig. 6, G–I.

Stratigraphic and geographic distribution: Araripe Basin, Santana Formation, Ceará State, Brazil, Aptian–Albian (Antonietto, 2010; Arai & Coimbra, 1990; Bate, 1972; Bate *et al.*, 2022; Bom *et al.*, 2021; Do Carmo *et al.*, 2008; Guzmán *et al.*, 2022; Melo *et al.*, 2020; Smith, 2000; Tomé *et al.*, 2014). Jatobá Basin, Pernambuco State, Brazil, Aptian (Tomé *et al.*, 2014). Parnaíba Basin, Codó Formation, Maranhão State, Brazil, Aptian (Barros *et al.*, 2022; Ramos *et al.*, 2006; this work).

Pattersoncypris symmetrica (Krömmelbein & Weber, 1971)
(Figure 3, G–I)

1971 *Hourcqia angulata symmetrica*: Krömmelbein & Weber, p. 81, Fig. 25, A–C.

CC BY

1990 *Hourcqia angulata symmetrica*: Silva-Telles & Viana, p. 318–321, Fig. 8.

2002 *Pattersoncypris angulata symmetrica*: Coimbra *et al.*, p. 691, Fig. 4, 30.

2008 *Harbinia symmetrica*: Do Carmo *et al.*, p. 795, Fig. 6, 9.

2010 *Harbinia symmetrica*: Antonietto, p. 25, Fig. 13, 1–8.

2012b *Kroemmelbeincypris symmetrica*: Poropat & Colin, p. 708, Fig. 4, 4.

2021 *Pattersoncypris symmetrica*: Araripe *et al.*, p. 6. Fig. 5, D–F.

2021 *Harbinia symmetrica*: Bom *et al.*, p. 5, Fig. 3, A–B.

2022 *Harbinia symmetrica*: Barros *et al.*, p. 5, Fig. 3, L.

2022 *Hourcqia angulata symmetrica*: Bate *et al.*, p. 79, Fig. 11, 5a–5c.

2022 *Pattersoncypris symmetrica*: Guzmán *et al.*, p. 11, Fig. 6, J–L.

Stratigraphic and geographic distribution: Gabon Basin, Gamba Formation, Gabon, Aptian. (Bate, 1999; Grosdidier, 1996). Congo Basin, Chela Formation, Congo, Aptian (Bate, 1999; Grosdidier, 1996). Araripe Basin, Santana Formation, Ceará State, Brazil, Aptian (Antonietto, 2010; Araripe *et al.*, 2021; Bom *et al.*, 2021; Coimbra *et al.*, 2002; Guzmán *et al.*, 2022; Silva-Telles Jr. & Viana, 1990). Parnaíba Basin, Codó Formation, Maranhão State, Brazil, Aptian (Barros *et al.*, 2022; Bate *et al.*, 2022; Do Carmo *et al.*, 2008; Krömmelbein & Weber, 1971; this work).

Pattersoncypris sp.
(Figure 3, J–L)

Author contributions

Lucas Lage Machado: conceptualization; investigation; data curation; writing – original draft; formal analysis; writing – review and editing; visualization. **Cecília de Lima Barros:** conceptualization; writing – review and editing; formal analysis. **Aristóteles de Moraes Rios-Netto:** conceptualization; writing – review and editing; project administration; supervision. **Benjamin Sames:** conceptualization; writing – review and editing; supervision. **Silvia Clara Silva:** conceptualization; writing – review and editing. **João Graciano Mendonça Filho:** conceptualization; writing – review and editing; formal analysis. **Joalice de Oliveira Mendonça:** conceptualization; writing – review and editing. **Danielle Marques-Lima:** conceptualization; writing – review and editing.

Conflict of interest

The authors declare no conflict of interest

Data availability statement

Data included in this study are publicly available in the literature or presented in the manuscript and supplementary files.

Funding information

This study was funded by the R&D project registered as "Projeto Alagoas: Correlação estratigráfica, evolução paleoambiental e paleogeográfica e perspectivas exploratórias do Andar Alagoas", sponsored by Shell Brasil Petróleo Ltda. as part of the "Compromisso com Investimentos em Pesquisa e Desenvolvimento" of Agência Nacional do Petróleo, Gás Natural e Biocombustíveis (ANP), technical cooperation agreement #20219.

Editor-in-chief

Dr. Claudine Dereczynski

Associate Editor

Dr. Hermínio Ismael de Araújo Júnior

How to cite:

Machado, L.L., Barros, C. L., Rios-Netto, A.M., Sames, B., Silva, S.C., Mendonça Filho, J.G., Mendonça, J.O., Marques-Lima, D. 2025, 'Biostratigraphy and Paleoenvironmental Characterization of the Lower Cretaceous Codó and Itapecuru Formations (Aptian–Albian, Parnaíba Basin, Brazil)', *Anuário do Instituto de Geociências,* 48:67620. https://doi.org/10.11137/1982-3908_2025_48_67620

CC BY